Modeling Dynamic Channel-Allocation Algorithms in Multi-BS TDD Wireless Networks With Internet-Based Traffic

William Cooper, *Student Member, IEEE*, James R. Zeidler, *Fellow, IEEE*, and Robert R. Bitmead, *Fellow, IEEE*

***Abstract*—Future time-division-duplex (TDD) systems operating over small wireless networks will utilize intelligent base station (BS)-coordinated dynamic channel-allocation algorithms in order to support high-bandwidth asymmetric traffic in adjacent cells. In this paper, we use extensive measurements of wireless Internet traffic from a large 802.11b network to create two random traffic models. One model, called "binomial," is memoryless and the other, called "dynamic," is based on an event-driven Markov state model with bidirectional flows and deterministic residence times. We then develop a two-BS two-zone wireless TDD interference model that describes the spatial features of interference between cochannel mobile stations (MSs) in adjacent BSs. This is a simplified precursor to more sophisticated models for multiple BSs and/or multisector BSs. We present a set of candidate TDD channel-allocation algorithms, which vary in their level of time-slot coordination and intelligent allocation between BSs. Lastly, we combine the three components (i.e., traffic models, interference models, and channel-allocation algorithms) to demonstrate the capacity for evaluating dynamic channel-allocation algorithms in realistic interference and Internet traffic scenarios. The results show that, for active MSs, the dynamic traffic model has a higher number of packet requests per time frame than the binomial traffic model, given the same mobile activity factor. Additionally, fixed channel-allocation algorithms generally perform much worse than pseudorandom and intelligent BS-coordinated algorithms, especially for asymmetric BSs. The pseudorandom algorithm performs well at low traffic, but suffers from severe interference blocking at high traffic. The intelligent BS-coordinated algorithm performs best, as it avoids MS-to-MS interference blocking from nearby users in adjacent cells and maximizes the overall throughput by attempting to allocate up- and downlink packet requests in corresponding time slots matched to the incoming uplink–downlink traffic demand for each time frame.**

***Index Terms*—Dynamic channel allocation, Internet traffic, time division duplex (TDD), WiFi, wireless networks.**

I. Introduction

THE demand for wireless mobile Internet access is driven by the continuing emergence of new multimedia services and applications, such as instant messaging, real-time media streaming, peer-to-peer file transfer, interactive gaming, etc., as well as by the introduction of ever smaller and more powerful wireless devices, such as personal digital assistants, two-way intelligent e-mail communicators, integrated web-camera servers, multimedia and game players, etc. Thus, the overall traffic characteristics for a wireless Internet network such as a 'WiFi' (i.e., IEEE 802.11b) system [1] can include a wide range of dynamic traffic properties (e.g., asymmetric up- and downlink message size, packet size, desired data rate and message latency, message-flow probability, etc.) that are dependent on the type of Internet service or application from each of the users on the network [2], [3] and the wireless terminal's capabilities. Additionally, the observed wireless Internet traffic message-arrival characteristics are quite different from the traditional Poisson-based call-arrival model, which has been widely used to characterize the voice traffic capacity for mobile cellular systems [4], [5]. These differences in traffic characteristics for the wireless Internet have a major impact on the packet capacity of an individual base station (BS) and the wireless network as a whole. Previously, in [6], the performance for multiple wireless web-browsing Internet users was optimized using polling resource-assignment algorithms with the aim to maximize the number of satisfied mobile stations (MSs) at a single BS, rather than any physical layer (e.g., radio-signal interference) considerations. This research investigates optimizing the overall wireless network throughput performance across multiple BSs simultaneously, with the goal of maximizing time-slot assignment while minimizing cochannel interference blocking.

Recently, wireless time-division-duplex (TDD) operating modes have been developed for third-generation networks, such as UTRA [7]–[9] and broad-band radio-access networks, such as HiperLAN2 [10]. TDD networks have a distinct advantage over frequency-division-duplex (FDD) networks for supporting these wireless Internet services, in that almost the entire transmission link (i.e., timeslots) can be dedicated to uplink (i.e., MS transmit) or downlink (i.e., MS receive) traffic. Also, the link capacity can be dynamically assigned on a per time frame basis to a single or plurality of users [11]. However, TDD networks suffer from a big disadvantage in that when multiple BSs are operating in close proximity to one another (as in a campus environment), significant levels of BS–BS and MS–MS (i.e., same-entity) interference can occur [12], in addition to the BS–MS and MS–BS (i.e., other-entity) interference that is normally experienced in multicellular FDD networks [13]. This same-entity interference is maximized

Manuscript received May 7, 2003; revised October 7, 2003 and December 25, 2003. This research was supported by Core Grant 02-10109, sponsored by Ericsson Wireless Communications, Inc., San Diego, CA.

W. Cooper and J. R. Zeidler are with the Electrical and Computer Engineering Department, University of California at San Diego, La Jolla, CA 92093-0407 USA (e-mail: wccooper@ece.ucsd.edu; zeidler@ece.ucsd.edu).

R. R. Bitmead is with the Department of Mechanical and Aerospace Engineering, University of California at San Diego, La Jolla, CA 92093-0411 USA (e-mail: rbitmead@ucsd.edu).

Digital Object Identifier 10.1109/TVT.2004.825776

when the uplink–downlink traffic ratios are asymmetric and the time slots are not coordinated between adjacent BSs.

Dynamic channel-allocation (DCA) schemes have been recently developed for FDD systems to mitigate inter- and intracell MS–BS interference by assigning users to predetermined physical channels, usually based on idle channel-signal level, some algorithms that consider factors such as mobility, user distribution, effect of handoffs, transmission delay [14]–[18], and, more recently, antenna arrays [19]. Similarly, packet-scheduling and transmission strategies for TDD systems have been proposed to reduce the transmission delay [20], maximize capacity [21], [22], and minimize overall interference [23].

This paper analyzes key conceptual issues and relationships between the instantaneous time-slot assignment and MS–MS interference-blocking performance (i.e., packet loss due to radio-signal interference) of various dynamic channel-allocation rules, traffic models, and spatial user distributions in two-BS wireless TDD networks. This analysis can then be expanded to encompass both multisector BSs and multi-BS networks.

Measured wireless Internet traffic from the University of California at San Diego (UCSD) campus-wide 802.11b wireless network is used to characterize the parameters for two random traffic models, known as "binomial" and "dynamic." In the binomial traffic model, which is stationary and memoryless, the users are characterized by their location, activity factor, and uplink–downlink packet-transmission ratio. In the dynamic model, an event-driven Markov process is developed to generate traffic streams for each user, where each active state is characterized by a bidirectional client–server message-flow sequence with predetermined message sizes. Independent Markov processes are then scaled up in parallel to create the overall instantaneous up- and downlink pseudo-Internet traffic for the desired number of users.

The wireless traffic streams from the binomial and dynamic models are then fed into two adjacent BSs using either "fixed," "pseudorandom," or "intelligent-coordinated" channel-allocation algorithms, which vary in their level of inter-BS coordination and corresponding performance. The fixed algorithm allocates time slots between BSs so as to avoid any MS cochannel interference, but does not optimize time-slot utilization. The pseudorandom algorithm ensures maximum time-slot allocation, but does not attempt to mitigate the MS–MS cochannel interference. The intelligent-coordinated algorithm optimizes both the time-slot allocation, as well as avoiding MS–MS cochannel interference.

The performance of the fixed and pseudorandom channel-assignment algorithms was then studied analytically for the binomial traffic model, but the treatment of the "intelligent BS-coordinated" channel-allocation algorithm with the dynamic traffic model was determined to be an NP-hard (i.e., nondeterministic in polynomial time) problem [24] and so was not attempted.

The rest of this paper is organized as follows. In Section II, the wireless Internet traffic measurements are described. In Section III, a two-BS MS location and cochannel interference model is described. In Section IV, stationary binomial and Markov-based dynamic traffic models for wireless Internet traffic are developed. In Section V, various channel-allocation algorithms (i.e., orthogonal, symmetric, pseudorandom, and intelligent) are explained and in Section VI the performance of orthogonal, symmetrical, and pseudorandom allocation algorithms are derived for stationary binomial traffic. In Section VII, the performance of the channel-allocation algorithms is simulated and discussed for both binomial and the equivalent dynamic traffic models. Lastly, Section VIII concludes this paper.

II. Wireless Internet Traffic Measurements

A. Wireless Internet Traffic Source

During 28 days in May 2002, aggregated Internet flow message logs were collected from the main Internet router for the entire campus-wide 802.11b network at UCSD, which at the time consisted of around 100 network access points, 3000 registered wireless Internet protocol (IP) addresses, and approximately 500 active users. (For more information on the current status of UCSD's Next Generation Network, see www.ngn.ucsd.edu.)

The dynamic characteristics of the UCSD 802.11b Internet traffic used in this paper were felt to be applicable to the analysis of DCA algorithms for the UMTS TDD mode for the following reasons.

a) *Wireless Data Rate*: 802.11b supports wireless data rates that are similar to the UMTS-TDD mode (11 Mb/s versus 2 Mb/s peak), so the same types of services and applications could be supported, e.g., web browsing, e-mail, file transfer, instant messaging, media streaming, etc.
b) *Network Configuration*: The UCSD 802.11b network consists of a large number of wireless access points in a campus environment, for both in-building and outside pico-cell-type pedestrian coverage. The UMTS-TDD mode is envisaged to support similar environments.

The aggregated Internet flow logs were collected in files, each representing 30 min intervals of flows. Overall, log data for approximately 377 GB of Internet message traffic from just over 16 million flows was collected, where a "flow" is defined as a self-contained independent entity of data carrying sufficient information to be routed from the source to the destination computer without reliance on earlier exchanges between this source and destination computer and the transporting network.

B. Flow Log Information

The Internet router traffic logs provided detailed information for each of the aggregated Internet flows. The information in the flow logs included the following.

1) *Source and Destination IP Address*: UCSD wireless network is allocated a range of discrete IP addresses (e.g., 128.54.xxx.xxx), which may be used to identify whether the flow originates (uplink) and/or terminates (downlink) in the UCSD wireless network.
2) *Source and Destination Port Address*: There are 65 535 Internet port numbers available, which are used to indicate the server application being accessed and the respective flow packet format. For most client–server applications, the source port for the client is chosen at

random from a range of reserved ports and the destination and source ports for the server is dependent on the specific Internet application (e.g., $\mathrm{HTTP} = \text{port } 80$, $\mathrm{FTP} = \text{port } 20$, Telnet $=$ port 23, Proxy Server $= 3128$, $\mathrm{DNS} = \text{port } 53$, etc.). This source and destination port information, along with the corresponding IP address and flow log-order information, can in many cases be used to tell whether the flow originated on a wireless client (e.g., a wireless web browser) or terminated in a wireless server (e.g., a website hosted on a wireless device). Exceptions to this include some peer-to-peer applications (e.g., Kazaa, etc.), where both source and destination can use the same port number.

3) *Number of Packets*: Each flow may consist of one or multiple packets segmented under the IP flow control. A packet is defined here as the unit of data that is routed between an origin and a destination on the Internet. In some Internet protocols [i.e., transmission control protocol (TCP)], individual packets are numbered and include the Internet destination address, so they can be routed around the Internet individually and reassembled into the original message at the destination.
4) *Flow Size*: Flow size (measured in bytes) indicates the total size of the overall flow from all the packets in the message including the retransmitted packets, but not including the overhead packets required for packet acknowledgment, flow and error control, etc. Given the number of packets in the flow and the flow size, the average packet size for each flow can be determined.
5) *Internet Protocol*: IP type indicates the message-flow protocol that is used. Three IP types are used for the majority of Internet flows.
    a) *TCP*: Connection-oriented protocol including packet sequencing, positive packet acknowledgment, error checksum, timeout and retransmit flow control, duplicate packet detection, long message segmentation into multiple packets, etc. The positive packet acknowledgment increases the overall flow-transmission time.
    b) *User Flow Protocol (UDP)*: Connectionless transport-layer protocol that, unlike TCP, adds no reliability, flow control, packet sequencing, or error-recovery functions to IP. Because of UDP's simplicity, UDP headers contain fewer bytes and consume less network overhead than TCP. UDP is useful in situations where the reliability mechanisms of TCP are not necessary, such as in cases where a higher layer protocol might provide error and flow control. UDP is the transport protocol for several well-known application-layer protocols, including network file system (NFS), simple network management protocol (SNMP), domain name system (DNS), and trivial file transfer protocol (TFTP), as well as some real-time applications, e.g., voice-over-IP, media streaming, multicasting, etc.
    c) *Internet Control Message Protocol (ICMP)*: Error-reporting and transmission-link diagnostics protocol that does not include any source or destination port information. One of the more common uses of UDP is send a "ping" (echo request) to an IP address and wait for the response, indicating the flow-routing and roundtrip propagation delay through the network.
6) *Interval*: Period in seconds between the arrival of the first and last packets in the aggregated flow, as measured at the router. Clearly, for a given packet-transmission route between the source IP address and the router, the fewer the number of packets in a flow and the smaller their size, the shorter is the interval.

C. Traffic-Measurement Limitations and Assumptions

Although the aggregate flow logs indicate the overall message size, they do not capture the exact message dynamics of the Internet link. For instance, as mentioned above, some Internet applications using UDP (such as some media-streaming applications) employ their own external flow control, long-message segmentation, packet-error correction, packet sequencing, and data-buffering mechanisms within their program code (i.e., independently of the IP layer) to avoid the packet delays inherent in TCP. Note that this application-based external flow-control mechanism creates multiple bidirectional flows per overall Internet flow. Similarly, the aggregated flow logs collected in this trace do not include any information about the size or number of packet-acknowledgment messages or the number of retransmitted packets contained within the flow. So, although some TCP and UDP applications may have similar overall message sizes, the aggregated flow logs do not accurately reflect their dynamic up- and downlink packet characteristics. Nevertheless, this is the appropriate level of aggregation to formulate and test DCA algorithms. Thus, due to this ambiguity and in order to simplify the analysis, it was decided to ignore the IP (i.e., TCP/UDP/ICMP) field information and the associated packet-flow-control mechanisms and dynamics and instead assume that all the flows were single contiguous packets. Also, it was assumed that individual message flows always originated in clients (e.g., web browsers, POP mail clients, etc.) and were immediately followed by message-flow responses in the opposite direction (i.e., originating in the corresponding server and terminating in the client). For peer-to-peer flows, the up- and downlink flows were assumed to be combined into corresponding pairs of flows, which may not exactly model the correct peer-to-peer flow sequence, but does not affect the overall traffic uplink–downlink byte ratio for the dynamic traffic model. Lastly, rather than creating a probability mass function (PMF) of the flow size for each Internet application type (i.e., port number) for the dynamic model, the message size was averaged over the measurements for each application.

TABLE I
SUMMARY OF WIRELESS INTERNET TRAFFIC-LOG MEASUREMENTS

Flow Direction	% of Total Flows	% of Total Bytes
Uplink (i.e. Tx)	45%	21%
Downlink (i.e. Rx)	41%	73%
Uplink & Downlink	4%	6%
Total Uplink	**47%**	**24%**
Total Downlink	**43%**	**76%**
Totals	**16 Million**	**377 GB**

Note the roughly equal percentage of up- and downlink flows, but asymmetric uplink-to-downlink byte ratio.

D. Traffic-Analysis Method

The approximately 16 million flow logs from the router were processed in the following manner.

1) *Sort Logs by IP Address*: Aggregated logs were separated by source and destination IP address. Three classes of files were generated for each 30-min collection interval.
   a) *Uplink Flows* ($\mathrm{SrcIP} = 128.54.xx.xxx$, $\mathrm{DestIP} \neq 128.54.xx.xxx$). These logs represent 802.11b uplink transmit messages.
   b) *Downlink Flows* ($\mathrm{SrcIP} \neq 128.54.xx.xxx$, $\mathrm{DestIP} = 128.54.xx.xxx$). These logs represent 802.11b downlink receive messages.
   c) *Uplink and Downlink Flows* ($\mathrm{SrcIP} = 128.54.xx.xxx$, $\mathrm{DestIP} = 128.54.xx.xxx$). These logs represent the same 802.11b message flow being received by the router from a wireless source, which is then transmitted back to the wireless network.

   By totaling the number and sizes of the flow message logs over all collected files, it was possible to determine the ratio of uplink-to-downlink traffic flows and bytes.
2) *Collate Logs by Port*: For each of the classes of files mentioned above, the logs were sorted by the source and destination port to determine the originating and terminating message logs for both wireless clients and wireless servers for each application, as per Section II-B.2) above. From this information, the total number of flows per application for wireless clients and servers and their respective average flow size was determined.

E. Traffic-Measurement Results Summary

The flow log measurements from the UCSD 802.11b wireless network are used to derive the parameters for the binomial and dynamic traffic models in order to evaluate the performance of some fixed and dynamic channel-assignment algorithms. The traffic measurements should not be regarded as anything other than a 28-day snapshot of the traffic on the wireless network, which is used to validate the dynamic channel-allocation evaluation framework. Future flow log measurements will certinly show different results as new services and applications become more prevalent (e.g., online gaming) and older services are phased out, (e.g., Napster). Our aim here is to develop a method. It is apparent how it might be amended to accommodate new traffic behavior.

TABLE II
LARGEST WIRELESS INTERNET APPLICATIONS (BYTES >1%)

Port	Application Name	% Total Bytes	Average Bytes Per Flow	% Total Flows
1214	Kazaa (Uplink)	3.28%	18,952	4.08%
	Kazaa (Downlink)	24.4%	130,813	4.32%
6346	Gnutella (Uplink)	4.06%	17,957	5.32%
	Gnutella (Downlink)	4.68%	19,837	5.56%
6699	Napster (Uplink)	0.96%	210,171	0.11%
	Napster (Downlink)	0.7%	219,387	0.08%
80	HTTP (Uplink)	1.06%	1,523	16.38%
	HTTP (Downlink)	19.46%	28,382	16.15%
3128	Proxy (Uplink)	2.97%	1,233	2.97%
	Proxy (Downlink)	1.84%	14,517	2.99%
2234	DirectPlay (Uplink)	0.22%	265,312	0.02%
	Directplay (Downlink)	3.18%	2,446,242	0.03%
20	FTP (Uplink)	0.19%	55,962	0.08%
	FTP (Downlink)	1.87%	538,954	0.08%
5190	AOL-IM/ICQ (Uplink)	0.45%	2,980	3.55%
	AOL-IM/ICQ (Downlink)	1.84%	3,835	3.67%
548	AppleTalk (Uplink)	3.60%	3,665,344	0.02%
	Appletalk (Downlink)	0.95%	935,742	0.02%
Totals Uplink		16.79%	10,827	32.53%
Total Downlink		58.92%	33,929	32.9%
Total Uplink & Downlink		75.71%		65.43%

Approximately 76% of the total traffic bytes were associated with applications that each had greater than 1% of the total traffic bytes. Note that these flow logs were collected in May 2002 and that Napster no longer operates as a file-sharing service.

Table I shows the total flows and traffic (in bytes) for the up- and downlink flow logs. Even though the percentage of transmit (Tx) and receive (Rx) flows is reasonably even (47% total uplink versus 43% total downlink), the total uplink traffic bytes are approximately one-third of the total downlink bytes (24% total uplink versus 76% total downlink). Note that the total uplink Rx bytes percentage (i.e., 76%) is used later, in Section IV, as the basis for the parameter β in the traffic models. As will be shown below, the imbalance in uplink–downlink traffic bytes is mainly due to the large percentage of the wireless Internet users who are downloading large files from nonwireless web hosts and peer-to-peer servers.

Table II below shows the largest up- and downlink applications that have greater than 1% of the total traffic bytes. The traffic was sorted by source and destination IP address and port number to determine the flow direction and application. These applications represent $\sim$66% of the total flows and $\sim$76% of the total bytes.

From Table II it can be seen that, in this measurement, the peer-to-peer file transfer applications (i.e., Kazaa, Gnutella, and Napster) represented approximately 40% of the bytes and 20% of the flows, whereas HTTP web browser access represented approximately 23% of the bytes and 40% of the total flows. This would suggest that the flows associated with the peer-to-peer file transfers (e.g., music, movies, etc.) were much larger than those associated with the wireless web access.

By sorting and collating individual flows by source and destination IP address and port number, the flows were then separated into up- and downlink flows for wireless clients and servers. The respective client "request" and server "response"

TABLE III
CLIENT AND SERVER APPLICATIONS WITH NORMALIZED FLOWS (BYTES >1%)

Port	Application Name	Average Uplink Size (Bytes)	Average Downlink Size (Bytes)	Normalized Flow %
1214	Kazaa (Client)	7,268	143,692	7.07%
	Kazaa (Server)	37,297	116,477	5.91%
6346	Gnutella (Client)	12,377	22,626	6.56%
	Gnutella (Server)	22,248	18,410	10.43%
6699	Napster (Client)	69,135	219,387	0.219%
	Napster (Server)	568,848	57,906	0.1%
80	HTTP (Client)	1,523	28,382	46.49%
	HTTP (Server)	64,356	270	4.19%
3128	Proxy (Client)	1,233	14,517	8.44%
	Proxy (Server)	2,162	15,377	0.09%
2234	DirectPlay (Client)	110,587	1,399,766	0.037%
	DirectPlay (Server)	265,312	3,116,422	0.053%
20	FTP (Client)	28,928	538,954	0.23%
	FTP (Server)	23,373,679	443,923	0.0003%
5190	AOL-IM/ICQ (Client)	348	3,835	10.07%
	AOL-IM/ICQ (Server)	8,351,772	3,906,697	0.003%
548	AppleTalk (Client)	3,665,334	949,107	0.066%
	AppleTalk (Server)	1,190,851	363,017	0.001
	Total flows to and from wireless clients (i.e. uplink requests and downlink responses)			79.21%
	Total flows to and from wireless servers (i.e. downlink requests and uplink responses)			20.79%

Note the roughly 1:4 ratio of flows associated with wireless servers versus those flows associated with wireless clients.

message sizes for the up- and downlink were then averaged and the flow percentages were normalized, as shown in Table III.

From the above averaged flow sizes and normalized flow percentages in Table III, it can immediately be seen that approximately 80% of the normalized flows are associated with wireless connected clients versus 20% associated with wireless servers. Also, the uplink flows from HTTP wireless clients (e.g., web page requests) are generally very small (average $= 1,523$ bytes) and that the corresponding downlink flows (e.g., web page responses) are much larger (average $= 28382$ bytes). The largest application of wireless "servers" was for peer-to-peer file transfer (e.g., Kazaa, Gnutella, etc.) with a total of about 16% of the flows. The other main source of wireless server flows was HTTP servers, i.e., users hosting web sites on wireless connected devices, such as laptops, etc. It was also expected that instant messaging (e.g., AOL-IM/ICQ) from wireless clients would have small average up- and downlink message sizes (348 and 3835 bytes, respectively), but it was not expected that wireless servers running AOL-IM/ICQ would have such large average up- and downlink message sizes (8.35 and 3.9 M bytes, respectively). We assume but did not confirm that this large message size resulted from a small number of users attaching large files to their messages. However, the flow percentage for AOL-IM/ICQ servers was so small as to be insignificant (0.003%), so this large message size was not investigated.

Given the above flow log measurements, equivalent binomial and dynamic traffic models can be created as follows.

III. TWO-BS INTERFERENCE MODEL

A two-BS two-zone TDD interference model was created to model the effects of interference in small wireless TDD networks, (such as in a campus-wide 802.11b system). The model describes the spatial features of interference between cochannel MSs in two adjacent BSs and was designed to isolate the factors underlying the time-slot assignment and interference-blocking probabilities. The model allows for a mathematical analysis of the performance of the channel-allocation algorithms with binomial traffic. This is a simplified precursor to more sophisticated models for multiple BSs and/or multisectored BSs.

Each BS consists of two regions known as "near" and "far," although more regions could have been assigned as appropriate to the interference model. The number of MSs in each region of a BS was defined as N_{near} and N_{far}. Up to one active MS in

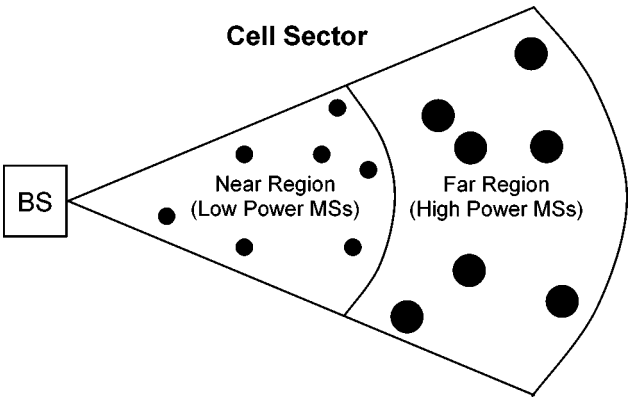

Fig. 1. User location and transmit power distribution model for simple two-region BS. N_{near} and N_{far} are the numbers of low and high power MSs in the "near" and "far" regions, respectively.

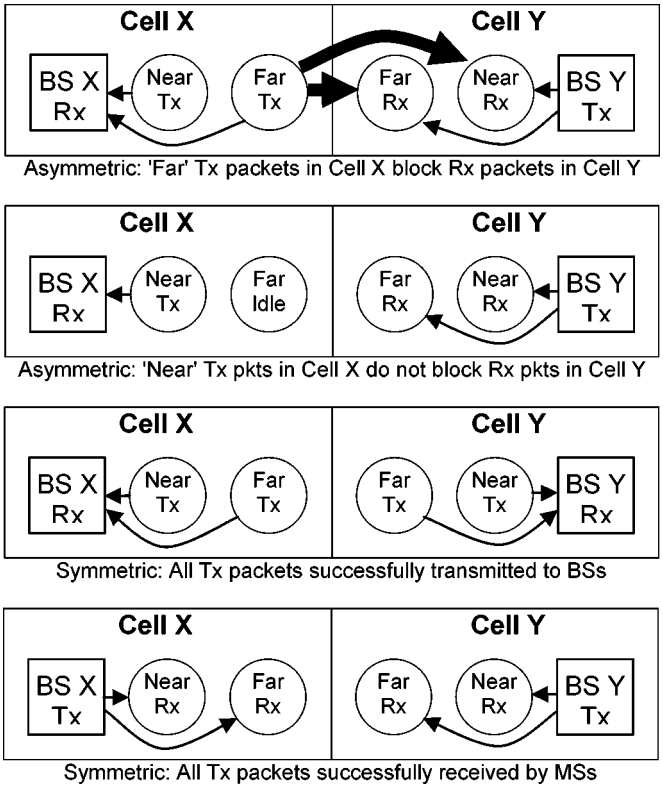

Fig. 2. Simple adjacent-cell interference model for a single time slot in a two-BS TDD network. MS transmit packet requests are always successfully transmitted to their respective BS. MS receive packets can be blocked by MS transmit packets in the far region of the adjacent cell.

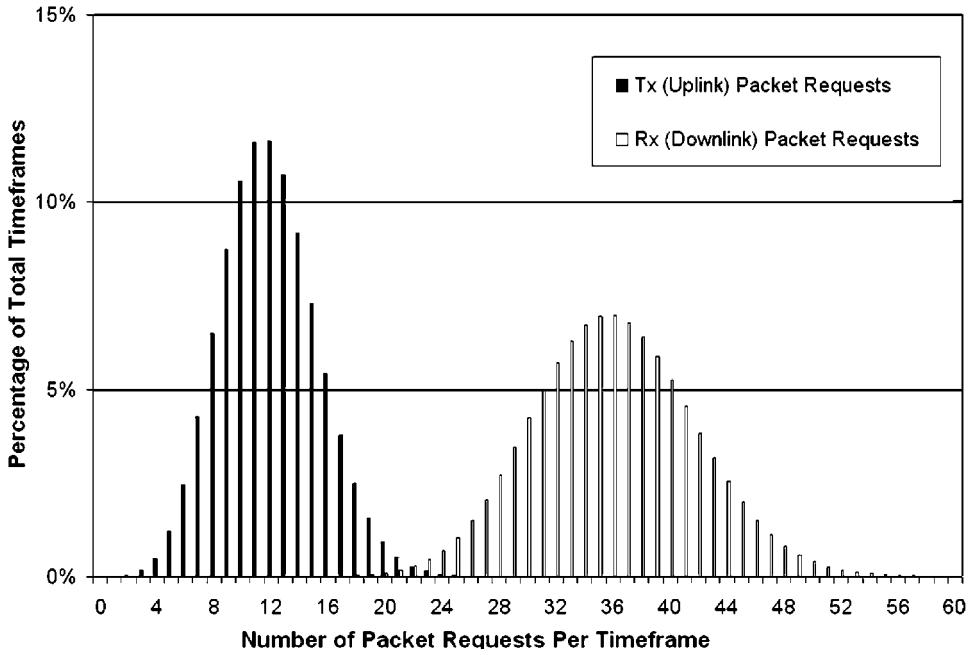

Fig. 3. Histograms of the total number of Tx and Rx packets generated per time frame from all MSs for binomially generated traffic, given $N = 48$ MSs, $T = 8$, $\beta = 0.75$, and $\alpha = 0.125$. Note that the mean total number of Tx and Rx packets per time frame $= 12$ and 36, respectively.

the near and/or far regions can be assigned by the BS to a time slot. Individual BSs ensure that any active MSs in the near or far region assigned to a time slot do not conflict with another MS in the corresponding region at that BS (i.e., either two transmit or two receive packets can be assigned to a time slot, but never a transmit and receive packet in the same time slot). MSs assigned to time slots in the near region transmit their packets at a low power level and MSs assigned to time slots in the far region transmit their packets at a high power level, as shown in Fig. 1.

Once assigned to a time slot, MS Tx packet requests are always successfully transmitted to their respective BSs, but MS Rx packets are only successfully received if they are not interference blocked by MS Tx packets assigned to the "far" (i.e., high-power) region of the adjacent (asymmetric) BS, as shown in Fig. 2.

Given the above assumptions for MS region assignment and the associated MS power levels and the simple rules for BS Rx interference blocking, the binomial and dynamic traffic models for each MS can now be defined.

IV. Binomial and Dynamic Traffic Models

The binomial and dynamic traffic models determine the number of Tx and Rx packet requests generated in a TDD time frame for each BS, based on the number of MS in the near and far BS regions, the number of time slots in a time frame, the MS activity factor, and the ratio of uplink (MS Tx) to downlink (MS Rx) packets, as determined from the wireless Internet traffic measurements described in Section II.

Whereas the purpose of the dynamic traffic model is to generate Internet traffic to simulate the performance of the wireless TDD network with various DCA algorithms, the purpose of the binomial traffic model is to analytically validate the DCA simulation model itself.

A. Binomial Traffic Model

In the binomial model, the MSs have a probability α of being active during a time slot and, given that a MS is active, then the MS has a probability β of being a Rx (i.e., downlink) packet. Thus, the probability that a transmit packet is generated by an individual MS during a time slot is given as

$$\Pr(X_{\text{Tx\_time slot}}) = (1-\beta)\alpha. \tag{1}$$

Similarly, the probability of a receive packet being generated by a MS during a time slot is given as

$$\Pr(X_{\text{Rx\_time slot}}) = \beta\alpha. \tag{2}$$

Given N_{near} users in the near region of a BS, the probability of having X_{Tx} packets generated in the near region over a time frame with T time slots is given by

$$\Pr(X_{\text{Tx\_near}}) = \binom{\text{TN}_{\text{near}}}{X_{\text{Tx}}} ((1-\beta)\alpha)^{X_{\text{Tx}}} \times (1-((1-\beta)\alpha))^{(\text{TN}_{\text{near}}-X_{\text{Tx}})}. \tag{3}$$

The corresponding histograms for the total number of Tx and Rx packets generated per time frame from all the MSs given the binomial traffic model with high traffic ($N = 48$) are shown in Fig. 3, where the value of β was chosen to approximately match the β of the UCSD traffic from Table I, i.e., $\beta = 0.75$.

Note that Fig. 3 represents the distribution of the total number of Tx and Rx packets generated per time frame by all the active MSs and not the distribution of the message lengths from the individual MSs. The message lengths for the binomial traffic model are exponentially distributed, i.e., the probability of X_{Rx} and X_{Tx} packets being generated sequentially by an individual MS equals $(\beta\alpha)^{X_{\text{Rx}}}$ and $((1-\beta)\alpha)^{X_{\text{Tx}}}$, respectively.

From Fig. 3, it can be observed that the mean number of Rx and Tx packets per time frame per region is 36 and 12, respectively (i.e., $\beta = 0.75$) and precise traffic measurements confirm this. The histograms are similar to Gaussian distributions and can be viewed as the sum of a large number of identically distributed binomial random variables (but are clearly limited in range between 0 and NT packets per time frame). Note that the probability of having zero Rx or Tx packets generated in a time frame is very small with the binomial traffic model in contrast to the dynamic traffic histograms shown later.

For those time frames when a Tx packet is generated by the binomial traffic model, the corresponding Tx packet request distribution is given from [26] and [27] by

$$\begin{aligned}&\Pr(X_{\mathrm{Tx}_{\mathrm{near}}}|X_{\mathrm{Tx}_{\mathrm{near}}} \geq 1)\\ &\quad = \binom{\mathrm{TN}_{\mathrm{near}} - 1}{X_{\mathrm{Tx}} - 1} ((1-\beta)\alpha)^{(X_{\mathrm{Tx}}-1)}\\ &\qquad \times (1 - ((1-\beta)\alpha))^{((\mathrm{TN}_{\mathrm{near}}-1)-(X_{\mathrm{Tx}}-1))}. \qquad (4)\end{aligned}$$

Similarly, the probability of a Tx packet being generated during a time frame with a total of X_{Tx} and X_{Rx} packets is given by

$$\begin{aligned}&\Pr(X_{\mathrm{Tx}}|X_{\mathrm{Tx}}, X_{\mathrm{Rx}})\\ &\quad = \binom{X_{\mathrm{Tx}} + X_{\mathrm{Rx}} - 1}{X_{\mathrm{Tx}} - 1} (\beta)^{X_{\mathrm{Rx}}} (1-\beta)^{(X_{\mathrm{Tx}}-1)}\\ &\qquad \cdot \binom{N_{\mathrm{near}}T - 1}{X_{\mathrm{Rx}} + X_{\mathrm{Tx}} - 1} (\alpha)^{(X_{\mathrm{Tx}}+X_{\mathrm{Rx}}-1)}\\ &\qquad \times (1-\alpha)^{(N_{\mathrm{near}}T - X_{\mathrm{Tx}} + X_{\mathrm{Rx}})}. \qquad (5)\end{aligned}$$

Equations for the corresponding Rx distributions are derived using the same equation forms.

Using the above model, four long series of integers (equivalent to at least 1 million time frames), representing the number of Tx and Rx packets per time frame in the near and far regions of a BS were generated and then fed into the various dynamic channel-allocation algorithms.

B. Dynamic Traffic Model

The dynamic traffic model is a Markov event-based state model with bidirectional flows and multiple states to represent the wireless client and wireless server applications for which the traffic distributed by the port types (in Table II) represented greater than 1% of the total bytes, as shown in Table IV.

The dynamic model uses the normalized flow percentages and average flow sizes from the UCSD 802.11b traffic measurements in Table III as the parameters for the different Markov states.

The "wireless client" states shown in Fig. 4 represented those states in which an uplink request flow was immediately followed by a downlink response flow. Similarly, the wireless server states represented those states in which a downlink request flow was immediately followed by an uplink response flow.

As an example of a state transition, given that an idle MS transitions to an active state, the probability P_1 of that MS going to state ① "Kazaa (Client)" is 7.07% (from Table III) and then the uplink Tx message flow size will be 7268 B immediately followed by a downlink Rx message of 143 692 B. The MS then returns to the "idle" state ⓪.

TABLE IV
DYNAMIC EVENT DRIVEN MARKOV MODEL STATES

State	P(x)	State Description	MS Tx or Rx (Uplink or Downlink)
Idle	P_0	Idle MS	-
Kazaa (Client)	P_1	Uplink Request Downlink Response	Tx Rx
Kazaa (Server)	P_{10}	Downlink Request Uplink Response	Rx Tx
Gnutella (Client)	P_2	Uplink Request Downlink Response	Tx Rx
Gnutella (Server)	P_{11}	Downlink Request Uplink Response	Rx Tx
Napster (Client)	P_3	Uplink Request Downlink Response	Tx Rx
Napster (Server)	P_{12}	Downlink Request Uplink Response	Rx Tx
HTTP (Client)	P_4	Uplink Request Downlink Response	Tx Rx
HTTP (Server)	P_{13}	Downlink Request Uplink Response	Rx Tx
Proxy (Client)	P_5	Uplink Request Downlink Response	Tx Rx
Proxy (Server)	P_{14}	Downlink Request Uplink Response	Rx Tx
DirectPlay (Client)	P_6	Uplink Request Downlink Response	Tx Rx
DirectPlay (Server)	P_{15}	Downlink Request Uplink Response	Rx Tx
FTP (Client)	P_7	Uplink Request Downlink Response	Tx Rx
FTP (Server)	P_{16}	Downlink Request Uplink Response	Rx Tx
AOL-IM/ICQ (Client)	P_8	Uplink Request Downlink Response	Tx Rx
AOL-IM/ICQ (Server)	P_{17}	Downlink Request Uplink Response	Rx Tx
AppleTalk (Client)	P_9	Uplink Request Downlink Response	Tx Rx
AppleTalk (Server)	P_{18}	Downlink Request Uplink Response	Rx Tx

Note that the event-driven states model a typical client–server flow for applications such as HTTP, FTP, etc. Peer-to-peer flows have been combined to fit the model, which does not affect the MS activity factor α or the Rx/total packets generated ratio β.

Peer-to-peer states (i.e., one-way flows) could have been created, but for expediency the corresponding up- and downlink peer-to-peer flows were paired to created pseudoclient and server states. This did not affect the ratio of uplink-to-downlink traffic or the number of peer-to-peer flows generated, just the dynamics with which the peer-to-peer flows were generated.

The Markov state-transition matrix for the event-driven dynamic traffic model (as shown in Fig. 5) is a 19 × 19 square matrix with the bottom 18 terms of the first column consisting of the normalized flow probabilities (from Table III) and the first row consisting of all ones except for the first term (i.e., in the first column), which is a zero.

From Fig. 5, the probability of being in state P_0 at time $(\mathrm{i}+1)$ is given by

$$P_{k(i+1)} = X_{k1}P_{1(i)} + X_{k2}P_{2(i)} + X_{k3}P_{3(i)} + , \ldots , + X_{km}P_{m(i)}. \qquad (6)$$

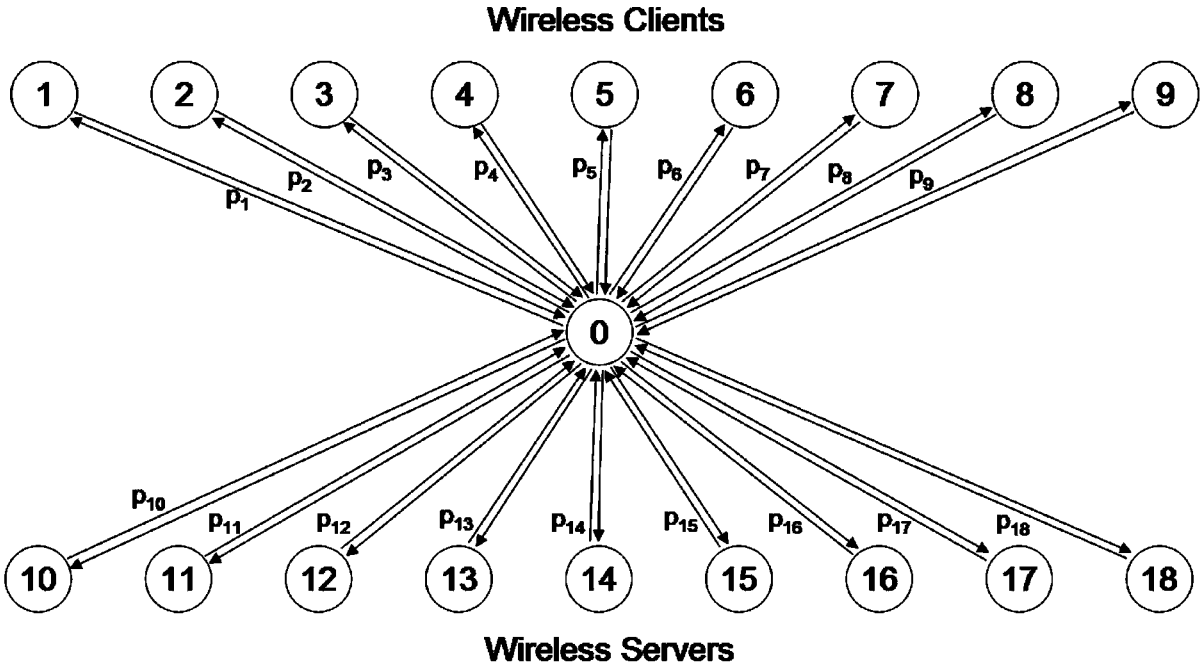

Fig. 4. Markov event-driven state diagram for the dynamic traffic model. Each transition to an active traffic state (see Table IV) starts in the idle state and has a client request flow followed by a server response flow back to the idle state.

$$
\begin{bmatrix} p_0 \\ p_1 \\ p_2 \\ p_3 \\ p_4 \\ p_5 \\ p_6 \\ p_7 \\ p_8 \\ p_9 \\ p_{10} \\ p_{11} \\ p_{12} \\ p_{13} \\ p_{14} \\ p_{15} \\ p_{16} \\ p_{17} \\ p_{18} \end{bmatrix}_{\substack{(i+1) \\ future\ state}}
=
\begin{bmatrix}
\overbrace{0}^{p_0} & \overbrace{1}^{p_1} & \overbrace{1}^{p_2} & \cdots & \cdots & \overbrace{1}^{p_{18}} \\
0.0707 & 0 & 0 & \cdots & \cdots & 0 \\
0.0591 & 0 & & & & 0 \\
0.0657 & & & & & \\
0.1043 & \vdots & & \ddots & & \vdots \\
0.0022 & & & & & \\
0.0010 & \vdots & & & & \vdots \\
0.4649 & & & & & \\
0.0419 & \vdots & & & & \vdots \\
0.0844 & & & \ddots & & \\
0.0009 & \vdots & & & & \vdots \\
0.0003 & & & & & \\
0.0005 & \vdots & & & & \vdots \\
0.0022 & & & & & \\
0.00002 & \vdots & & & & \vdots \\
0.1077 & & & & \ddots & \\
0.00003 & \vdots & & & & \vdots \\
0.0006 & 0 & & & & 0 \\
0.00001 & 0 & 0 & \cdots & \cdots & 0
\end{bmatrix}
\cdot
\begin{bmatrix} p_0 \\ p_1 \\ p_2 \\ p_3 \\ p_4 \\ p_5 \\ p_6 \\ p_7 \\ p_8 \\ p_9 \\ p_{10} \\ p_{11} \\ p_{12} \\ p_{13} \\ p_{14} \\ p_{15} \\ p_{16} \\ p_{17} \\ p_{18} \end{bmatrix}_{\substack{(i) \\ current\ state}}
$$

Fig. 5. State-transition matrix for finite state Markov process. Note that all the columns sum to 1.

Note that each state returns to the idle state P_0 with probability 1. Additional states could have been added to represent the probabilities that client requests and server replies did not get successfully received. The Markov states are also modulated with a probability α to indicate whether the MS is active (i.e., Tx or Rx packets) or inactive (i.e., idle time slots).

The Markov state probabilities and associated flow sizes dictate the resulting β for the dynamic traffic model. From Table III, it can easily be shown that the average (i.e., the expectation of the) uplink (Tx) and downlink (Rx) flow sizes are 14 295 and 40 344 B respectively, given a mobile activity factor $\alpha = 1$. Thus, the theoretical β of the dynamic model is $40344/(14,295 + 40344) = 0.74$, which corresponds very

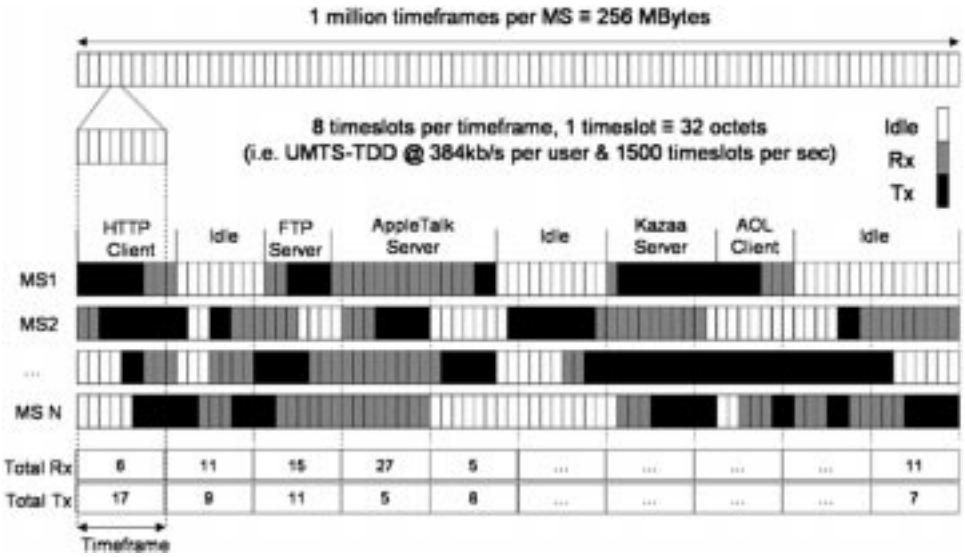

Fig. 6. Markov dynamic traffic generator. The total number of near and far Tx and Rx packets per BS from all the active MSs is calculated for each time frame. This dynamic traffic data is then fed into the DCA algorithms.

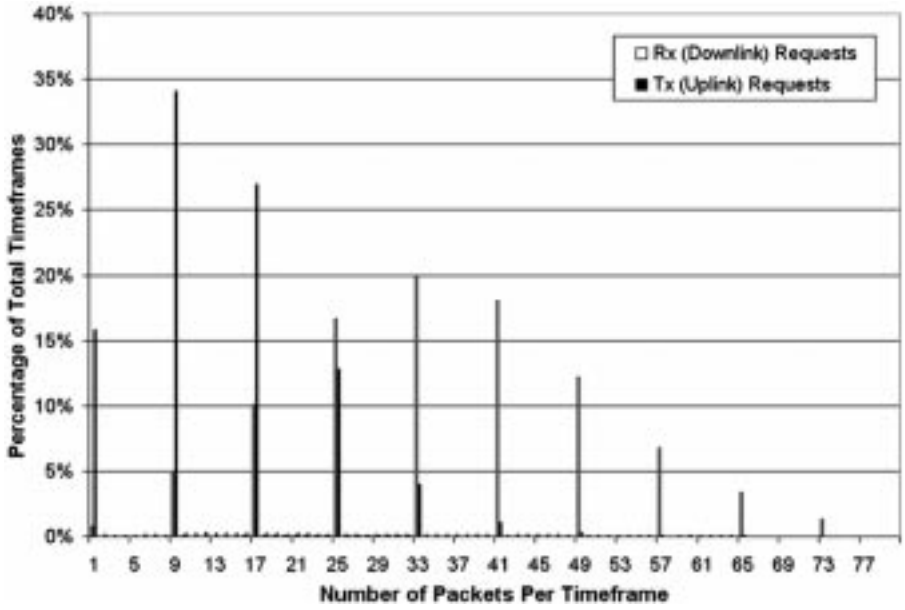

Fig. 7. Histograms of the total Tx and Rx packets per time frame generated by all the MSs at a BS using the dynamic traffic model, given $N = 48$ MSs, $T = 8$, $\beta \approx 0.75$ (measured), $\alpha = 0.125$. Note that the short spikes are due to some MS message lengths not being an exact multiple of the time frame length. Compare these histograms with those in Fig. 3, which utilize the same N, T, α, and β and result in the same mean total number of Tx and Rx packets per time frame (i.e., 12 and 36, respectively).

closely with the measured β_{UCSD} of the UCSD 802.11 traffic in Table I, i.e., 0.76.

In this investigation, the traffic channel model was based upon an eight time-slot system with each user able to transmit at 384 kb/s (e.g., one of the UMTS-TDD data rates) and 1500 time slots per second, so each time slot is equivalent to 32 B. Fig. 6 shows the Tx and Rx packet-request flows generated for N users, with the users starting in state 0 and transitioning to any of the wireless client or server states and back to (the idle) state 0 and repeating the process until the array equivalent to 256 MB is filled with Tx, Rx, or idle time slots. The Tx and Rx packets generated by the dynamic model are then summed for each time frame over all the MSs and for the near and far regions of each BS.

Using the above Markov-state-based traffic model, the simulated up- and downlink flows and idle periods for each user were generated and measured. The measurements of the total number of Tx and Rx packets generated by the dynamic traffic model over 1 M time frames (i.e., 256 MB) resulted in values of $\beta_{\mathrm{DYNAMIC}} = 0.757$, $\alpha_{\mathrm{DYNAMIC}} = 0.128$, and $(N_{\mathrm{near}}/N_{\mathrm{TOTAL}})_{\mathrm{DYNAMIC}} = 0.5048$, which validates the output statistics of the dynamic traffic model.

Additional measurements were used to create histograms of the total number of Tx and Rx packet requests generated (in the near and far regions) per time frame by all the MSs, as shown in Fig. 7, for the high traffic case (i.e., $N = 48$).

BS Region	Allowable Request Permutations							Invalid Permutations			
	I	II	III	IV	V	VI	VII				
Near	Tx	Tx	Idle	Idle	Rx	Rx	Idle	2Tx	Rx	Tx	Rx
Far	Tx	Idle	Tx	Idle	Rx	Idle	Rx	Tx	2Rx	Rx	Tx

Fig. 8. Allowable BS time-slot assignments. Multiple or opposing allocations are not allowed.

		Permutation Number											
		1	2	3	4	5	6	7	8	9	...	...	49
BS 1	Near	Tx	Tx			Rx		Rx	Tx	Tx	...	...	Idle
	Far	Tx		Tx			Rx	Rx	Tx		...	...	Idle
BS 2	Far	Tx	Tx	Tx	Tx	Tx	Tx	Tx	Tx	Tx	...	...	Idle
	Near	Tx	Tx	Tx	Tx	Tx	Tx	Tx			...	...	Idle
BS 1 Throughput		2Tx	1Tx	1Tx	Ø	0	0	0	2Tx	1Tx	...	...	Ø
BS 2 Throughput		2Tx	2Tx	2Tx	2Tx	2Tx	2Tx	2Tx	1Tx	1Tx	...	...	Ø

Fig. 9. Channel assignments throughputs for 49 possible time-slot assignments.

It should be noted that the histograms in Fig. 7 do not represent the distribution of the Tx and Rx flow sizes. Instead, the corresponding up- and downlink flow sizes for each Markov state in the dynamic traffic model are given in Table III.

From the histograms in Figs. 3 and 7, it can be observed that the dynamic and binomial traffic models have approximately the same mean total Tx and Rx packets generated per time frame (i.e., approximately 12 and 36 packets, respectively) and, indeed, the dynamic model was measured to have the an average of 12.82 Tx and 35.17 Rx packets per time frame (given the parameters in Fig. 7), which corresponds with the $\beta \approx 0.75$. Similarly, the dynamic traffic model was measured to have a MS activity factor $\alpha = 0.125$.

It can be seen in Fig. 7 that the histogram peaks are spaced at increments of the number of time slots per time frame (i.e., $T = 8$), indicating that the flow sizes for each MS are much larger than the number of bytes per time frame (i.e., 256 bytes). The peaks at 0 packets per time frame represent those time frames when no MSs are active and the peaks spaced at k^*T packets per time frame represent those time frames when k MSs are active during that time frame. Note that there are some very small spikes ($<$2%) with non-T packet spacing, which indicate those time frames where the messages end and the message length was not an exact multiple of the time-frame length.

It is interesting to observe in Fig. 7 that even with $N = 48$ MSs and the large flow sizes generated by the dynamic traffic model, there is a high percentage of time frames with no Tx packets generated (i.e., $\sim$16%).

C. Assumptions and Limitations of the Traffic Models

In order to keep the analysis and simulation of the channel-allocation algorithms tractable, the binomial and dynamic models were designed to be as simple as possible. This simplification is acceptable as long as the traffic-model assumptions are understood and do not affect the assessment of the dynamic channel-allocation algorithms.

1) Limitations of the Binomial Traffic Model.
   a) *Arrivals process*: The binomial process does not model bursty packet arrivals from multiple MSs. Rather, it assumes that each mobile is identically distributed in its packet generation probability (i.e., α), so the number of active mobiles per time slot is exponentially distributed.
   b) *Packet Generation*: The binomial model is a memoryless process and does not create server/client message-flow sequences. The binomial process generates active receive packets according to known probabilities (i.e., α and β) without respect to their order of generation.
   c) *Message Length*: The binomial traffic model has an exponentially distributed message size for each user, rather than a long-tailed distribution as seen in some Internet traffic measurements (e.g., Pareto and self-similar traffic models [3], [25]).
2) Limitations of the Dynamic Traffic Model.
   a) *Message Length*: Message length is fixed to the average measured message length (in Table III) rather than some long-tailed distribution that is more representative of actual Internet traffic.
   b) *Single-Packet Messages*: Messages are assumed to be contained in a single aggregated flow, rather than segmented into multiple packets, as with long messages in TCP/IP. The flow control, packet acknowledgment, and error-correction flows are not reflected in the Markov model.
   c) *Markov Model*: The Markov model assumes a number of parallel users each with their own single traffic state at any instant in time. The Markov model implemented does not support multiple data streams from individual users, e.g., simultaneous file download and web-page access.
   d) *NP-Hard Problem*: Theoretical analysis of the various channel-allocation algorithms with the

		Permutation Number											
		1	2	3	4	5	6	7	8	9	...	...	49
BS 1	Near	Tx	Tx			Rx		Rx	Tx	Tx		...	Idle
	Far	Tx		Tx			Rx	Rx	Tx			...	Idle
BS 2	Far	Tx	Tx	Tx	Tx	Tx	Tx	Tx	Tx	Tx		...	Idle
	Near	Tx	Tx	Tx	Tx	Tx	Tx	Tx				...	Idle

Fig. 10. Allowable pseudorandom assignments. Conflicting assignments are allowed, so assignment blocking is minimized, but interference blocking is experienced.

Markov based dynamic traffic model was determined to be an NP-hard (i.e., nondeterministic in polynomial time) problem [24], so the calculation of the throughput of the channel-allocation algorithms with the dynamic model is limited to simulations.

Given these assumptions and limitations, the traffic models are applied to the various dynamic channel-allocation algorithms.

V. Channel Allocation

A. Allowable Time-Slot-Assignment Permutations

The channel-allocation algorithms have some basic rules that are independent, of which channel-allocation algorithm is used as shown in Fig. 8. First, only one packet can be assigned in the near or far regions of a BS per time slot. Second, any time slot can be allocated to Tx or Rx packet requests, but not both.

B. Channel-Assignment Throughput

Fig. 9 shows some of the possible permutations for a two-BS system.

Given these possible packet-assignment permutations, some rules about packet throughput can be deduced.

1) Tx Throughput:
   - 100% regardless of any packets at the corresponding time slot at the adjacent BS.
2) Rx Throughput:
   - 100% if an Rx or Idle packet is in the far region of the corresponding time slot at an adjacent BS.
   - 0% if a Tx packet is in the far region of the corresponding time slot at the adjacent BS.

Four channel-allocation algorithms were investigated in this paper, as follows:

1) Pseudorandom Allocation (no time-slot coordination or inter-BS communications);
2) Orthogonal Allocation (open-loop time-slot coordination without inter-BS communications);
3) Symmetrical Allocation (open-loop time-slot coordination without inter-BS communications);
4) Intelligent Dynamic Channel Allocation (closed-loop intelligent time-slot coordination via BS communication).

These algorithms are described below.

C. Pseudorandom Allocation

Allocation Rule: Assign Rx and Tx packets to time slots independently of the other BS and of the Rx/Tx packet ratio for each time frame at that BS and without trying to align or order packets within the time frames. Thus, the probabilities of assigning Tx or Rx packets to a time slot are equal, (i.e., 0.5). Some of the allowable permutations for pseudorandom assignment are shown in Fig. 10.

		Timeslot Number							
		1	2	3	4	5	6	7	8
BS 1	Near		Rx		Tx		Rx		Tx
	Far		Rx		Tx		Rx		Tx
BS 2	Far	Rx		Tx		Rx		Tx	
	Near	Rx		Tx		Rx		Tx	

Fig. 11. Orthogonal channel assignments. No interference blocking is experienced, but assignment blocking is severe.

Since all assigned transmit packets are received correctly, the transmit throughput with pseudorandom channel assignment in binomial traffic is equivalent to the corresponding transmit packet-assignment probability. Also, there is no attempt to avoid adjacent BS interference and the Rx throughput is dependent on the Tx packet assignment in each time frame at the adjacent BS (see Section V-B and Fig. 2).

D. Orthogonal Allocation

Allocation Rule: Assign discrete time slots for each BS to transmit and receive, such that there is no packet activity in the corresponding time slot at the adjacent BS, as shown in Fig. 11.

The packet throughput is dependent on the uplink–downlink ratio at the BS, as an equal number of time slots are assigned to transmit and receive packets. Thus, the throughput is very inefficient in asymmetric traffic, although the assignment minimizes inter-BS interference, since all users are orthogonal between BSs.

E. Symmetric Allocation

Allocation Rule: Assign equal numbers of receive and transmit time slots for corresponding packets at both BSs, as shown in Fig. 12.

The intelligent coordinated-BS channel-allocation algorithm is optimal in the sense that it attempts to maximize the overall throughput of the two adjacent BSs independent of the traffic model, but it is by no means the only algorithm that may achieve this level of throughput. Indeed, there are many other algorithms that have other desired allocation characteristics, which have

		Timeslot Number							
		1	2	3	4	5	6	7	8
BS 1	Near	Tx	Rx	Tx	Rx	Tx	Rx	Tx	Rx
	Far	Tx	Rx	Tx	Rx	Tx	Rx	Tx	Rx
BS 2	Far	Tx	Rx	Tx	Rx	Tx	Rx	Tx	Rx
	Near	Tx	Rx	Tx	Rx	Tx	Rx	Tx	Rx

Fig. 12. Symmetric channel assignments. No interference blocking is experienced and all time slots are assigned, given sufficient traffic.

not been considered here. The flow diagram for the intelligent coordinated-BS assignment algorithm is shown in Fig. 13.

The up- and downlink traffic must be symmetric at the BSs to achieve optimal capacity. There is increased "MS to other BS" physical layer interference over the interleaved orthogonal case, since twice as many time slots are allocated for traffic, although in this simple model the "MS to other BS" physical layer interference is not reflected in the channel throughput rules.

F. Intelligent Coordinated-BS Allocation

The intelligent coordinated-BS allocation algorithm consists of a series of allocation rules that are performed in strict order and are designed to:

- maximize the overall number of packets that can be packed into the time frame at both BSs by attempting to match the maximum number of corresponding Tx or Rx packets at both BSs and then allocating them to time slots;
- avoid MS-to-MS interference between adjacent BSs, as shown in Fig. 2, by only allowing allocation of
  - corresponding Tx or Rx packets at both BSs;
  - Rx packet(s) at one BS with a Tx packet in the near region at the other BS;
  - pairs of or single Tx or Rx packets at one BS;
- improve the traffic-load balancing across both BSs by assigning time slots to single corresponding packets at both BSs before allocating a matching pair of packets at one BS;
- approximately match the Tx/Rx packet allocation to the β of the time frame, where the number of Tx or Rx packets allocated to a time slot at both BSs could achieve the same packet throughput.

The allocation rules in the intelligent coordinated-BS algorithm are executed in order from a) to g) for each time frame until all the packets are allocated or all of the time slots are assigned, whichever comes first.

A possible assignment sequence is shown in Fig. 14, although for illustration purposes, there are more than eight time slots allocated.

The intelligent coordinated-BS channel-allocation algorithm can easily be modified to operate in a multi-BS multisector environment, given an appropriate interference-blocking model, as shown by Fig. 2 for the case of the simple two-BS network). In a multi-BS multisector network, the allocation algorithm has to be adjusted to avoid the possibility of interference blocking between adjacent sectors within a single BS and between sectors in adjacent BSs. Thus, new allocation rules need to be es-

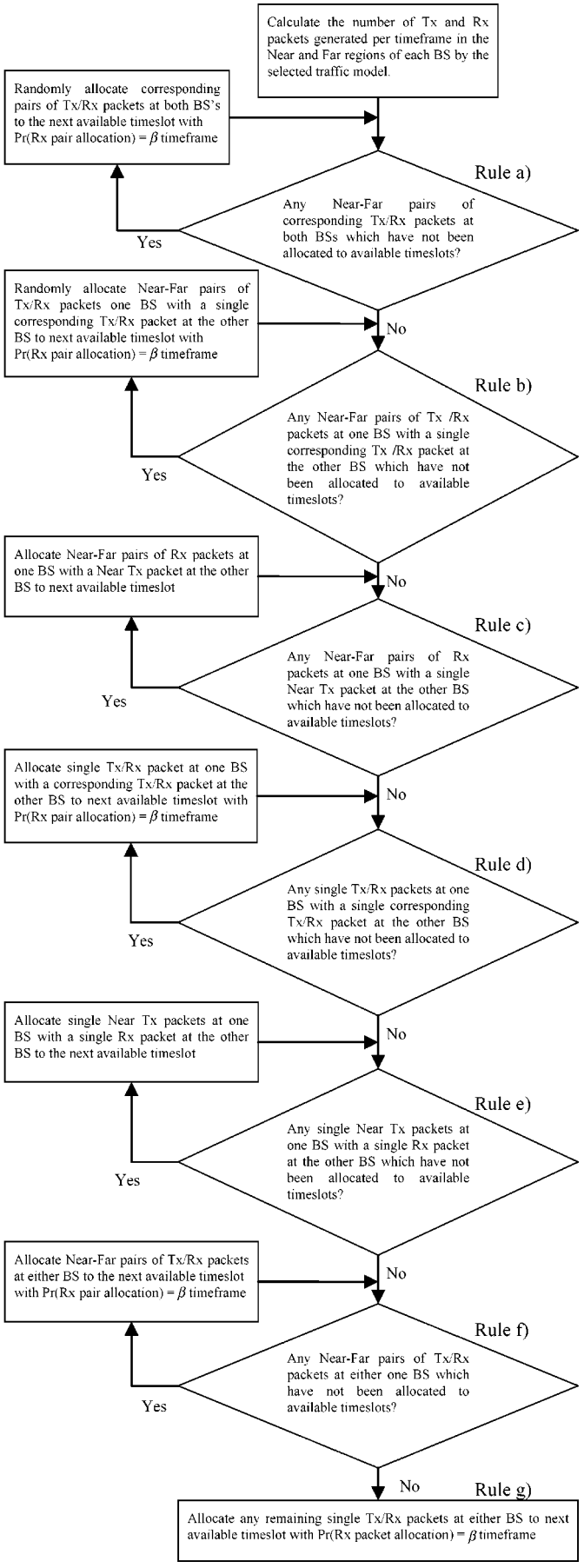

Fig. 13. Flow diagram for intelligent coordinated-BS channel allocation.

		Intelligent Coordinated-BS Channel Allocation										
Timeslot		1	2	3	…	…	…	…	...	...	…	T
BS 1	Near	Rx	Tx	Rx	Tx	Tx	Rx	Tx	Tx			
	Far	Rx	Tx		Tx				Tx	Tx		Tx
BS 2	Far	Rx	Tx	Rx		Rx	Rx	Rx			Rx	
	Near	Rx	Tx	Rx	Tx	Rx						
Rule		a)	a)	b)	b)	c)	d)	e)	f)	g)	g)	g)

Fig. 14. Example of possible intelligent coordinated-BS channel assignment for a time frame with T time slots. Note that time-slot assignment blocking is minimized and interference blocking is avoided.

tablished that utilize a larger number of geographically defined areas within each BS sector. The effect of these additional geographically defined areas and associated allocation rules is to reduce the number of permissible time-slot allocation combinations, which reduces the packet-assignment rate. Clearly, as the number of adjacent sectors increases, so the packet assignment efficiency degrades. Thus, the intelligent coordinated-BS allocation algorithm works best on small TDD systems.

VI. Theoretical Throughput With Binomial Traffic

Given the time-slots assignment algorithm and the binomial packet-generation model, the throughput can be derived for all cases except the intelligent coordinated-BS algorithm, where it was determined that the number and complexity of the rules made a theoretical analysis impractical.

A. Pseudorandom Throughput

1) Transmit Throughput With Pseudorandom Allocation: As mentioned previously, the Tx packet throughput is equivalent to the Tx packet-assignment probability. Assuming that both near and far regions for each BS are assigned (as in the high-traffic case), the probability of A_{Tx} packets being assigned given that X_{Rx} receive and X_{Tx} transmit packets are generated in a time frame with T time slots is given by the hypergeometric distribution shown in (7) at the bottom of the page.

Substituting in (7) for the probability of generating X_{Tx} and X_{Rx} packet requests, given that a Tx packet is generated from (5), we get the equation for the transmit throughput with pseudorandom channel allocation as

$$\begin{aligned}
&\Pr(\text{Tx_Throughput_Pseudorandom}) \\
&\quad= \sum_{A_{\mathrm{Tx}}=1}^{T} \sum_{X_{\mathrm{Tx}}=A_{\mathrm{Tx}}}^{\mathrm{NT}} \sum_{X_{\mathrm{Rx}}=0}^{\mathrm{NT}-X_{\mathrm{Tx}}} \left(\frac{A_{\mathrm{Tx}}}{X_{\mathrm{Tx}}}\right) \\
&\qquad\times \Pr(X_{\mathrm{Tx}}, X_{\mathrm{Rx}} | X_{\mathrm{Tx}} \geq 1) \\
&\qquad\times \Pr(A_{\mathrm{Tx}} | X_{\mathrm{Tx}}, X_{\mathrm{Rx}}) \\
&\quad= \sum_{A_{\mathrm{Tx}}=1}^{T} \sum_{X_{\mathrm{Tx}}=A_{\mathrm{Tx}}}^{\mathrm{NT}} \sum_{X_{\mathrm{Rx}}=0}^{\mathrm{NT}-X_{\mathrm{Tx}}} \left(\frac{A_{\mathrm{Tx}}}{X_{\mathrm{Tx}}}\right) \\
&\qquad\times \frac{\binom{X_{\mathrm{Tx}}}{A_{\mathrm{Tx}}} \binom{X_{\mathrm{Rx}}}{\min\{X_{\mathrm{Rx}}, T-A_{\mathrm{Tx}}\}}}{\binom{X_{\mathrm{Tx}}+X_{\mathrm{Rx}}}{A_{\mathrm{Tx}}+\min\{X_{\mathrm{Rx}}, T-A_{\mathrm{Tx}}\}}} \\
&\qquad\times \binom{X_{\mathrm{Rx}}+X_{\mathrm{Tx}}-1}{X_{\mathrm{Tx}}-1} (1-\beta)^{(X_{\mathrm{Tx}}-1)} (\beta)^{(X_{\mathrm{Rx}})} \\
&\qquad\times \binom{\mathrm{NT}-1}{X_{\mathrm{Rx}}+X_{\mathrm{Tx}}-1} (\alpha)^{(X_{\mathrm{Rx}}+X_{\mathrm{Tx}}-1)} \\
&\qquad\times (1-\alpha)^{(\mathrm{NT}-X_{\mathrm{Rx}}-X_{\mathrm{Tx}})}. \qquad (8)
\end{aligned}$$

2) Receive Throughput With Pseudorandom Allocation: Calculating the receive-packet throughput requires knowledge of both adjacent BSs' pseudorandom channel allocation. The assigned receive packets get successfully received if the corresponding time slot in the other BS also contains a receive packet, an unused time slot, or a transmit packet in the near region. A receive packet will be interference blocked by a transmit packet at the corresponding time slot in the far region of the adjacent BS. Again, we assume that both the near and far regions are assigned as in the high-traffic case.

Thus, the probability of successfully receiving S_{Rx} packets at BS1 with pseudorandom allocation is given by

$$\begin{aligned}
&\Pr(\text{Tx_Assignment_Pseudorandom}) \\
&= \begin{cases}
\dfrac{\binom{X_{\mathrm{Tx}}}{A_{\mathrm{Tx}}} \binom{X_{\mathrm{Rx}}}{\min\{X_{\mathrm{Rx}}, T-A_{\mathrm{Tx}}\}}}{\binom{X_{\mathrm{Tx}}+X_{\mathrm{Rx}}}{A_{\mathrm{Tx}}+\min\{X_{\mathrm{Rx}}, T-A_{\mathrm{Tx}}\}}}, & \begin{cases} X_{\mathrm{Rx}} > 0 \\ A_{Tx_{\min}} = \begin{cases} X_{\mathrm{Tx}} & X_{\mathrm{Tx}}+X_{\mathrm{Rx}} \leq T \\ T-X_{\mathrm{Rx}}, & X_{\mathrm{Tx}}+X_{\mathrm{Rx}} > T \end{cases} \\ A_{Tx_{\max}} = \begin{cases} X_{\mathrm{Tx}}, & X_{\mathrm{Tx}} \leq T \\ T, & X_{\mathrm{Tx}} > T \end{cases} \end{cases} \\
0, & \begin{cases} X_{\mathrm{Rx}} = 0 \\ A_{\mathrm{Tx}} < T \\ X_{\mathrm{Tx}} \neq A_{\mathrm{Tx}} \end{cases} \\
1, & \begin{cases} X_{\mathrm{Rx}} = 0 \\ A_{\mathrm{Tx}} = T \\ X_{\mathrm{Tx}} \geq A_{\mathrm{Tx}} \end{cases}
\end{cases}. \qquad (7)
\end{aligned}$$

$$\begin{aligned}&\Pr(\text{Rx\_Throughput\_Pseudorandom})\\&=\sum_{k=1}^{T}\Pr(S_{\text{Rx\_BS1}}=k)\\&=\sum_{k=1}^{T}\sum_{A_{\text{Rx\_BS1}}=k}^{T}\sum_{A_{\text{Tx\_BS2}}=0}^{T-k}\\&\quad\times\left(\Pr(A_{\text{Rx\_BS1}})\Pr(A_{\text{Tx\_BS2}})\right.\\&\qquad\left.\times\Pr(S_{\text{Rx\_BS1}}=k|A_{\text{Rx\_BS1}},A_{\text{Tx\_BS2}})\right).\end{aligned}\tag{9}$$

Given that A_{Rx} and A_{Tx} packets are assigned to time slots in BS1 and BS2, respectively, the probability that S_{Rx} receive packets are successfully received at BS1 is given by the hypergeometric distribution as shown in (10) at the bottom of the page.

The probability of assigning $A_{\text{Rx\_BS1}}$ receive packets at BS1 given that a receive packet is generated at BS1, is given by

$$\begin{aligned}&\Pr(A_{\text{Rx\_BS1}}=k)\\&=\sum_{X_{\text{Tx\_BS1}}=0}^{\text{NT}-X_{\text{Rx}}}\sum_{X_{\text{Rx\_BS1}}=k}^{\text{NT}}\\&\quad\times\left(\frac{\Pr(A_{\text{Rx\_BS1}}=k|X_{\text{Rx\_BS1}},X_{\text{Tx\_BS1}})}{X_{\text{Rx\_BS1}}}\right.\\&\qquad\left.\times\Pr(X_{\text{Rx\_BS1}}|X_{\text{Rx\_BS1}},X_{\text{Tx\_BS1}})\right).\end{aligned}\tag{11}$$

Note that in (11) the probability of assigning k receive packets is normalized by the number of receive packets generated (i.e., $X_{\text{Rx\_BS1}}$) in order to calculate the throughput per receive packet generated at BS1.

Similar to the transmit throughput case (7), the probability of A_{Rx} packets being assigned time slots as BS1 given X_{Rx} and X_{Tx} packets being generated, i.e., $\Pr(A_{\text{Rx\_BS1}}|X_{\text{Rx\_BS1}},X_{\text{Tx\_BS1}})$, is a hypergeometric distribution given by (12) at the bottom of the page.

The probability of assigning $A_{\text{Tx\_BS2}}$ transmit packets at BS2 is given by

$$\begin{aligned}&\Pr(A_{\text{Tx\_BS2}}=k)\\&=\sum_{X_{\text{Tx\_BS2}}=k}^{\text{NT}}\sum_{X_{\text{Rx\_BS2}}=0}^{\text{NT}-X_{\text{Tx\_BS2}}}\\&\quad\times\left(\Pr(A_{\text{Tx\_BS2}}=k|X_{\text{Tx\_BS2}},X_{\text{Rx\_}}BS2)\right.\\&\qquad\left.\times\Pr(X_{\text{Tx\_BS2}},X_{\text{Rx\_BS2}})\right)\end{aligned}\tag{13}$$

where the probability of assigning $A_{\text{Tx\_BS2}}$ transmit packets at BS2 given X_{Tx} and X_{Rx} packets at BS2, i.e., $\Pr(A_{\text{Tx\_BS2}}|X_{\text{Tx\_BS2}},X_{\text{Rx\_BS2}})$ is identical to the form given in (12).

Now that the Rx and Tx packet-assignment probabilities have been defined for BS1 and BS2, respectively, the probability of generating X_{Rx} receive packets in a time frame containing $X_{\text{Tx}}+X_{\text{Rx}}$ packet requests (i.e.,

$$\begin{aligned}&\Pr(\text{Successful\_Rx}_{\text{BS1}}\text{\_Pseudorandom})\\&=\frac{\binom{A_{\text{Tx}_{\text{far}}\text{\_BS2}}}{A_{\text{Rx\_BS1}}-S_{\text{Rx}}}\binom{T-A_{\text{Tx}_{\text{far}}\text{\_BS2}}}{S_{\text{Rx}}}}{\binom{T}{A_{\text{Rx\_BS1}}}},\\&\begin{cases}S_{\text{Rx}_{\min}}=\begin{cases}0 & A_{\text{Tx\_BS2}}\geq A_{\text{Rx\_BS1}}\\A_{\text{Rx\_BS1}}-A_{\text{Tx\_BS2}} & A_{\text{Tx\_BS2}}<A_{\text{Rx\_BS1}}\end{cases}\\S_{\text{Rx}_{\max}}=\begin{cases}A_{\text{Rx\_BS1}} & T-A_{\text{Tx\_BS2}}\geq A_{\text{Rx\_BS1}}\\T-A_{\text{Rx\_BS2}} & T-A_{\text{Tx\_BS2}}<A_{\text{Rx\_BS1}}\end{cases}\end{cases}.\end{aligned}\tag{10}$$

$$\begin{aligned}&\Pr(\text{Assign\_Rx\_Pseudorandom})\\&=\begin{cases}\dfrac{\binom{X_{\text{Rx}}}{A_{\text{Rx}}}\binom{X_{\text{Tx}}}{\min\begin{cases}X_{\text{Tx}}\\T-A_{\text{Rx}}\end{cases}}}{\binom{X_{\text{Rx}}+X_{\text{Tx}}}{\min\begin{cases}A_{\text{Rx}}+X_{\text{Tx}}\\T\end{cases}}}, & \begin{cases}X_{\text{Tx}}>0\\A_{\text{Rx}_{\min}}=\begin{cases}X_{\text{Rx}} & X_{\text{Tx}}+X_{\text{Rx}}\leq T\\T-X_{\text{Tx}} & X_{\text{Tx}}+X_{\text{Rx}}>T\end{cases}\\A_{\text{Rx}_{\max}}=\begin{cases}X_{\text{Rx}} & X_{\text{Rx}}\leq T\\T & X_{\text{Rx}}>T\end{cases}\end{cases}\\0, & \begin{cases}X_{\text{Tx}}=0\\A_{\text{Rx}}<T\\X_{\text{Rx}}\neq A_{\text{Rx}}\end{cases}\\1, & \begin{cases}X_{\text{Tx}}=0\\A_{\text{Rx}}=T\\X_{\text{Rx}}\geq A_{\text{Rx}}\end{cases}\end{cases}.\end{aligned}\tag{12}$$

$\Pr(X_{\text{Rx\_BS1}}|X_{\text{Rx\_BS1}}, X_{\text{Tx\_BS1}})$ from (11) can be obtained. First, we need to derive the probability of generating a receive packet in a time frame where X_{Rx} receive packets are generated, which is given by

$$\begin{aligned}&\Pr(X_{\text{Rx}}|X_{\text{Rx}} \geq 1)\\ &= \sum_{X_{\text{ACTIVE}}=X_{\text{Rx}}}^{\text{NT}} \binom{X_{\text{ACTIVE}}-1}{X_{\text{Rx}}-1} (\beta)^{(X_{\text{Rx}}-1)}\\ &\quad \times (1-\beta)^{(X_{\text{ACTIVE}}-X_{\text{Rx}})}\\ &\quad \times \binom{\text{NT}-1}{X_{\text{ACTIVE}}-1} (\alpha)^{(X_{\text{ACTIVE}}-1)}\\ &\quad \times (1-\alpha)^{(\text{NT}-X_{\text{ACTIVE}})}. \end{aligned} \tag{14}$$

The probability of generating a receive packet in a time frame containing $X_{\text{Tx}} + X_{\text{Rx}}$ packet requests is then given by

$$\begin{aligned}&\Pr(X_{\text{Rx}}|X_{\text{Rx}}, X_{\text{Tx}})\\ &= \binom{X_{\text{Rx}}+X_{\text{Tx}}-1}{X_{\text{Rx}}-1} (\beta)^{(X_{\text{Rx}}-1)} (1-\beta)^{(X_{\text{Tx}})}\\ &\quad \times \binom{\text{NT}-1}{X_{\text{Rx}}+X_{\text{Tx}}-1} (\alpha)^{(X_{\text{Rx}}+X_{\text{Tx}}-1)}\\ &\quad \times (1-\alpha)^{(\text{NT}-X_{\text{Rx}}-X_{\text{Tx}})}\\ &1 \leq X_{\text{Rx}}\\ &1 \leq X_{\text{Rx}} + X_{\text{Tx}} \leq \text{NT}. \end{aligned} \tag{15}$$

Finally, substituting (10) – (13) and (15) back into (9) and applying the appropriate limits, we get the equation for the receive throughput with pseudorandom allocation in binomial traffic.

B. Orthogonal Throughput

The transmit packet throughput in the near region with orthogonal channel allocation and binomial traffic is given as

$$\begin{aligned}&\Pr(\text{Tx\_Throughput\_near\_Orthogonal})\\ &= \sum_{X_{\text{Tx}}=1}^{\frac{T}{4}} (P_{X_{\text{Tx-near}}}) + \sum_{X_{\text{Tx}}=\left(\frac{T}{4}+1\right)}^{N_{\text{near}}T} (P_{X_{\text{Tx-near}}}) \left(\frac{\left(\frac{T}{4}\right)}{X_{\text{Tx}}}\right)\\ &= \sum_{X_{\text{Tx}}=1}^{\frac{T}{4}} \binom{\text{TN}_{\text{near}}-1}{X_{\text{Tx}}-1} ((1-\beta)\alpha)^{(X_{\text{Tx}}-1)}\\ &\quad \times (1-((1-\beta)\alpha))^{((\text{TN}_{\text{near}}-1)-(X_{\text{Tx}}-1))}\\ &= \sum_{X_{\text{Tx}}=\left(\frac{T}{4}+1\right)}^{N_{\text{near}}T} \binom{\text{TN}_{\text{near}}-1}{X_{\text{Tx}}-1} ((1-\beta)\alpha)^{(X_{\text{Tx}}-1)}\\ &\quad \times (1-((1-\beta)\alpha))^{((TN_{\text{near}}-1)-(X_{\text{Tx}}-1))} \left(\frac{\left(\frac{T}{4}\right)}{X_{\text{Tx}}}\right). \end{aligned} \tag{16}$$

The transmit packet throughput in the far region with orthogonal channel allocation and binomial traffic are derived in a similar manner.

The overall transmit packet throughput with orthogonal channel allocation is then given by

$$\begin{aligned}&\Pr(\text{Tx\_Througput\_Overall\_Orthogonal})\\ &= \frac{N_{\text{near}}}{N} \Pr(\text{Tx\_Througput\_near\_Orthogonal})\\ &\quad + \frac{N_{\text{far}}}{N} \Pr(\text{Tx\_Througput\_far\_Orthogonal}). \end{aligned} \tag{17}$$

The Rx throughput results for orthogonal allocation and binomial traffic are obtained following the same process as with the Tx throughput case.

C. Symmetric Throughput

The transmit packet throughput in the near region with symmetric channel allocation and binomial traffic is given as

$$\begin{aligned}&\Pr(\text{Tx\_near\_Symmetrical})\\ &= \sum_{X_{\text{Tx}}=1}^{\frac{T}{2}} (P_{X_{\text{Tx-near}}}) + \sum_{X_{\text{Tx}}=\left(\frac{T}{2}+1\right)}^{N_{\text{near}}T} (P_{X_{\text{Tx-near}}}) \left(\frac{\left(\frac{T}{2}\right)}{X_{\text{Tx}}}\right)\\ &= \sum_{X_{\text{Tx}}=1}^{\frac{T}{2}} \binom{\text{TN}_{\text{near}}-1}{X_{\text{Tx}}-1} ((1-\beta)\alpha)^{(X_{\text{Tx}}-1)}\\ &\quad \times (1-((1-\beta)\alpha))^{((TN_{\text{near}}-1)-(X_{\text{Tx}}-1))}\\ &\quad + \sum_{X_{\text{Tx}}=\left(\frac{T}{2}+1\right)}^{N_{\text{near}}T} \binom{\text{TN}_{\text{near}}-1}{X_{\text{Tx}}-1} ((1-\beta)\alpha)^{(X_{\text{Tx}}-1)}\\ &\quad \times (1-((1-\beta)\alpha))^{((\text{TN}_{\text{near}}-1)-(X_{\text{Tx}}-1))} \left(\frac{\left(\frac{T}{2}\right)}{X_{\text{Tx}}}\right). \end{aligned} \tag{18}$$

Similarly, the transmit packet throughput in the far region with symmetric channel allocation and binomial traffic is derived in a similar manner.

The overall BS Tx throughput with symmetric channel allocation in binomial traffic is then given by

$$\begin{aligned}&\Pr(\text{Tx\_Througput\_Symmetrical\_Overall})\\ &= \frac{N_{\text{near}}}{N} \Pr(\text{Tx\_Througput\_near\_Symmetrical})\\ &\quad + \frac{N_{\text{far}}}{N} \Pr(\text{Tx\_Througput\_far\_Symmetrical}). \end{aligned} \tag{19}$$

The Rx throughput results for symmetric allocation and binomial traffic are obtained following the same process as with the Tx throughput case.

VII. Simulation Results and Discussion

The results in this section show simulated throughputs from the four dynamic channel-allocation algorithms with binomial and dynamic traffic. Note that the theoretical results exactly match the simulated results for the symmetric, orthogonal, and pseudorandom allocation algorithms with binomial traffic.

Before the results are discussed, it is first necessary to derive the number of packets generated per time frame at low and high traffic levels by the binomial and dynamic traffic models.

The binomial traffic model at low traffic levels (i.e., $N_{\text{total}} = 4$) generates an average of four packet requests per time frame (i.e., $\text{E}[X_{\text{total}}] = N_{\text{total}} T\alpha = 4 * 8 * 0.125 = 4$). Given that $N_{\text{near/far}} = 0.5$ and $\beta = 0.75$, this is

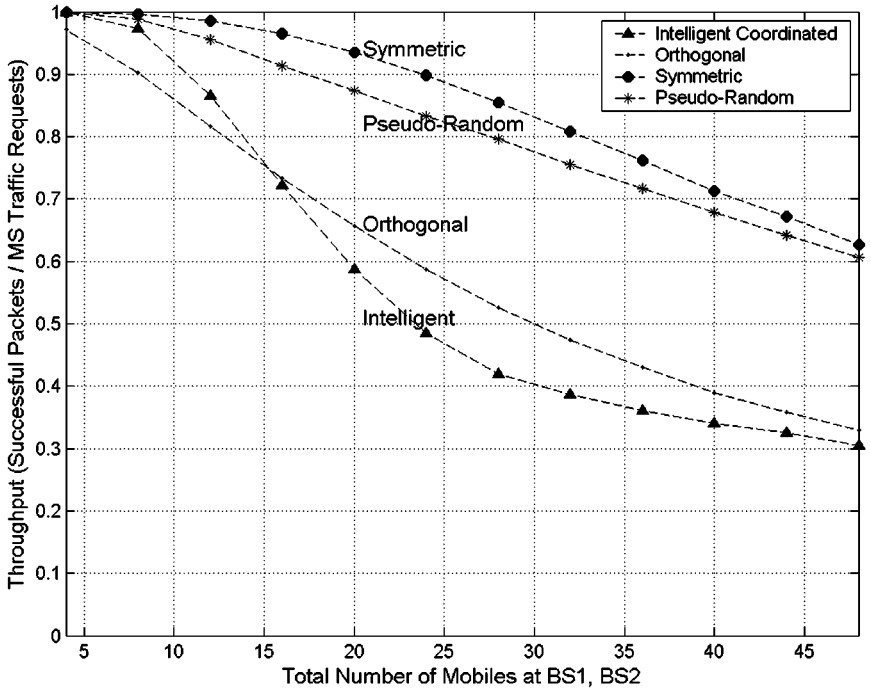

Fig. 15. Tx throughput with various channel-allocation methods in binomial traffic. $\alpha = 0.125$, $\beta = 0.75$, $N_{\rm near}/N_{\rm far} = 0.5$, $T = 8$, and time frame trials = 100 000. Note that the intelligent coordinated-allocation algorithm has the worst Tx throughput as single Tx packets in the far region are purposely limited (i.e., unassigned) to reduce adjacent BS Rx interference blocking.

equivalent to $\mathrm{E}[X_{\rm Tx\_near}] = \mathrm{E}[X_{\rm Tx\_far}] = 0.5$, $\mathrm{E}[X_{\rm Rx\_near}] = \mathrm{E}[X_{\rm Rx\_far}] = 1.5$.

Similarly, at high traffic levels (i.e., $N_{\rm total} = 48$), the binomial traffic model generates an average of 48 packet requests per time frame (i.e., $\mathrm{E}[X_{\rm total}] = \mathrm{N}_{\rm total}T\alpha = 48 * 8 * 0.125 = 48$). Given that $N_{\rm near/far} = 0.5$ and $\beta = 0.75$, this is equivalent to $\mathrm{E}[X_{\rm Tx\_near}] = \mathrm{E}[X_{\rm Tx\_far}] = 6$, $\mathrm{E}[X_{\rm Rx\_near}] = \mathrm{E}[X_{\rm Rx\_far}] = 18$, as shown in Fig. 3.

For the dynamic model, the average number of packets per time frame is the same as with the binomial model, but the dynamic model exhibits the following characteristics:

1) very large numbers of packets generated per time frame (i.e., T, $2T$, $3T$, etc., due to the large flow sizes compared with the small number of time slots per time frame (as observed by the large spikes in Fig. 7);
2) small number of packets per time frame, which corresponds to those flows that are not an exact multiple of the number of time slots per time frame (as observed by the very small non-T–spaced spikes in Fig. 7);
3) no packets generated at all (as observed in Fig. 7 by the spikes showing ∼16% and ∼1% of time frames without any Tx and Rx packets, respectively).

A. Tx Throughput with Binomial Traffic

At low traffic levels, it can be seen in Fig. 15 that the throughput with the binomial traffic model is high for all allocation algorithms. This is because at low traffic levels only a small number of Tx packets are generated per time frame (i.e., $\mathrm{E}[X_{\rm Tx\_near}] = 0.5$) and there are sufficient time slots with all channel-allocation algorithms to allow nearly all the packet requests to be assigned.

At high traffic levels, i.e., $\mathrm{E}[X_{\rm Tx\_near}] = \mathrm{E}[X_{\rm Tx\_far}] = 6$, the following can be observed about the Tx throughput with binomial traffic:

1) symmetric throughput is approximately 0.64, which is reasonable since only four time slots are available at the near and far regions for Tx allocation, (i.e., $4/6 = 0.66$);
2) orthogonal throughput is approximately 0.33, since only half as many time slots (i.e., 2) are available for Tx allocation compared to the symmetric algorithm (i.e., $2/6 = 0.33$);
3) pseudorandom throughput is approximately 0.61 (note that the pseudorandom and symmetric allocation have approximately the same throughput at high traffic levels, as the pseudorandom algorithm assigns Tx packets to time slots with a 0.5 probability (see Section V-C) and the symmetric algorithm allocates 50% of the time slots to Tx packets, so when the channel is saturated the Tx throughput of both algorithms is about the same);
4) intelligent coordinated-BS throughput is approximately 0.3, as it limits the number of Tx packets assigned in the far region (see Fig. 13 and Rules C and E) to avoid Tx interference blocking at the adjacent BS.

B. Rx Throughput With Binomial Traffic

In Fig. 16, the Rx throughput is again high at low traffic levels (i.e., $\mathrm{E}[X_{\rm Rx\_near}] = \mathrm{E}[X_{\rm Rx\_far}] = 1.5$) for all allocation algorithms as few packets are generated per time frame with the binomial model and most of the Rx packets are assigned time slots.

At high traffic levels, i.e., $\mathrm{E}[X_{\rm Rx\_near}] = \mathrm{E}[X_{\rm Rx\_far}] = 18$, the following can be observed in Fig. 16 about the Rx throughput with binomial traffic:

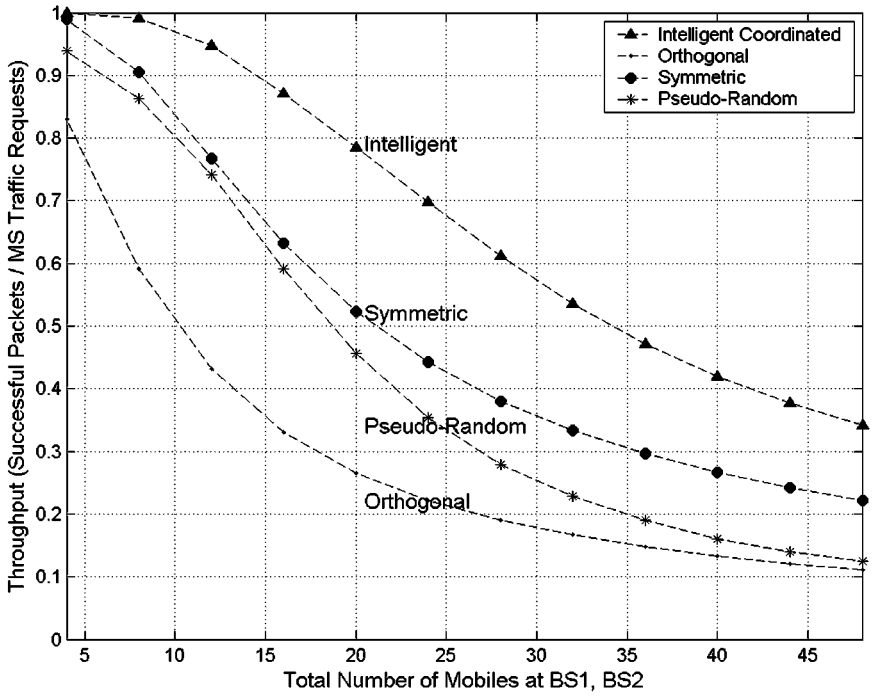

Fig. 16. Rx throughput with various channel-allocation methods in binomial traffic. $\alpha = 0.125$, $\beta = 0.75$, $N_{\rm near}/N_{\rm far} = 0.5$, $T = 8$, and time frame trials $= 100\,000$. Note that the intelligent coordinated-allocation algorithm has the best Rx throughput, as the Rx packet assignment is roughly proportional to β with some Rx bias and the adjacent BS Rx interference blocking is avoided by limiting Tx assignment where appropriate.

1) symmetric throughput is approximately 0.22, which corresponds to $\mathrm{T}/2 = 4$ time slots allocated to Rx packets and 18 Rx packets generated in each region;
2) orthogonal throughput performs the worst at 0.11, which is half the symmetric throughput, as half as many time slots $(\mathrm{T}/4 = 2)$ are allocated to meet the Rx traffic demand and the channel saturates;
3) pseudorandom throughput is very poor as the Tx:Rx packet assignment is uniform (see Section V-C) and the Rx packets are blocked by interference from Tx packets in the corresponding time slots at the adjacent BS;
4) intelligent coordinated-BS throughput is highest of all the allocation algorithms at 0.35, as the algorithm biases the allocation of Rx packet requests (see Fig. 13 and Rules C and E).

C. Overall Throughput With Binomial Traffic

The overall BS throughput in binomial traffic is shown in Fig. 17. At low traffic levels, all the channel-allocation algorithms have good throughput performance. At high traffic levels, when the channel is saturated, the following can be observed about the overall throughput in binomial traffic:

1) symmetrical throughput is approximately 0.33, which corresponds to 16 packets (eight time slots for the near and far regions) assigned out of an average of 48 packets generated per time frame;
2) orthogonal throughput is approximately 0.17, approximately half of the symmetric algorithm throughput, as the orthogonal algorithm allocates only half of the time slots to traffic;
3) pseudorandom throughput is high at low traffic levels, but the algorithm suffers from significant Tx interference blocking at high traffic levels;
4) intelligent coordinated-BS throughput is the best at all traffic levels as it maximizes the packet allocation and avoids Tx interference blocking.

Note the throughputs of the intelligent coordinated-BS and symmetric algorithms converge at high traffic levels, as the channels saturate when all the available time slots are filled. Thus, at high traffic levels any algorithm that allocates all of the time slots and avoids interference blocking is optimal.

D. Tx Throughput With Dynamic Traffic

Fig. 18 shows the Tx throughput in dynamic traffic. The following can be observed about the Tx throughput at low traffic levels:

1) symmetric throughput is approximately 0.5, as given $N_{\rm total} = 4$, (i.e., $N_{\rm near} = N_{\rm far} = 2$); even if one MS is active, the number of packets generated per time frame is twice the number of time slots allocated to Tx traffic and the channel is saturated;
2) orthogonal throughput is approximately 0.25, (i.e., half the symmetric throughput) as only T/4 time slots are allocated to Tx traffic and the channel is saturated; this channel saturation at all traffic levels with the dynamic model explains why the throughput function is much flatter for the symmetric and orthogonal allocations, as shown in Fig. 18;
3) pseudorandom throughput is about 0.85, as the algorithm allows all the time slots to be assigned;

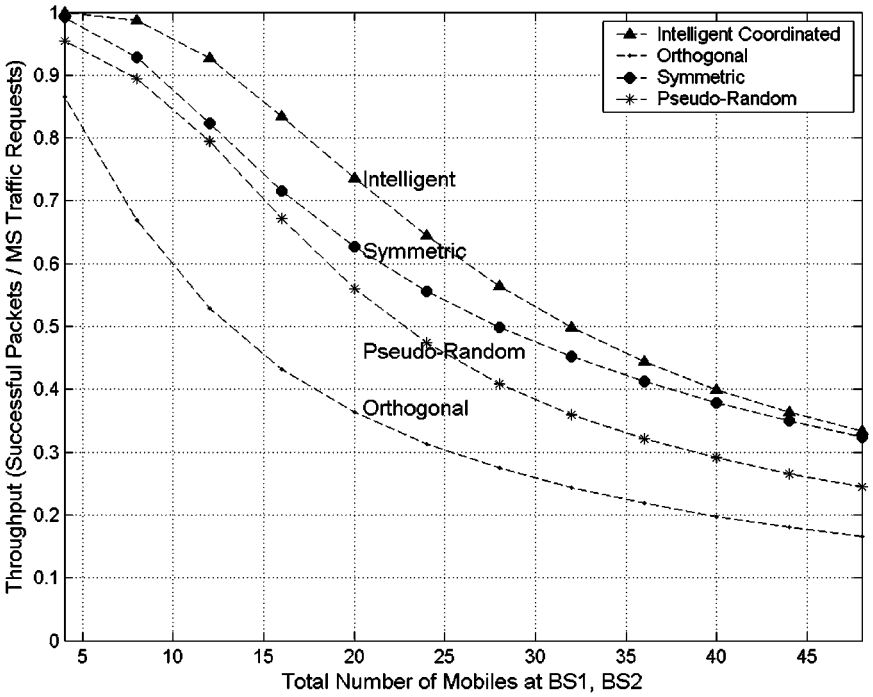

Fig. 17. Overall throughput of BS with various channel-allocation methods in binomial traffic. $\alpha = 0.125$, $\beta = 0.75$, $N_{\rm ncar}/N_{\rm far} = 0.5$, $T = 8$, and time frame trials $= 100\,000$. The intelligent coordinated-allocation algorithm has the best overall throughput, as the maximum number of packets are allocated to the time slots and Tx interference blocking is avoided.

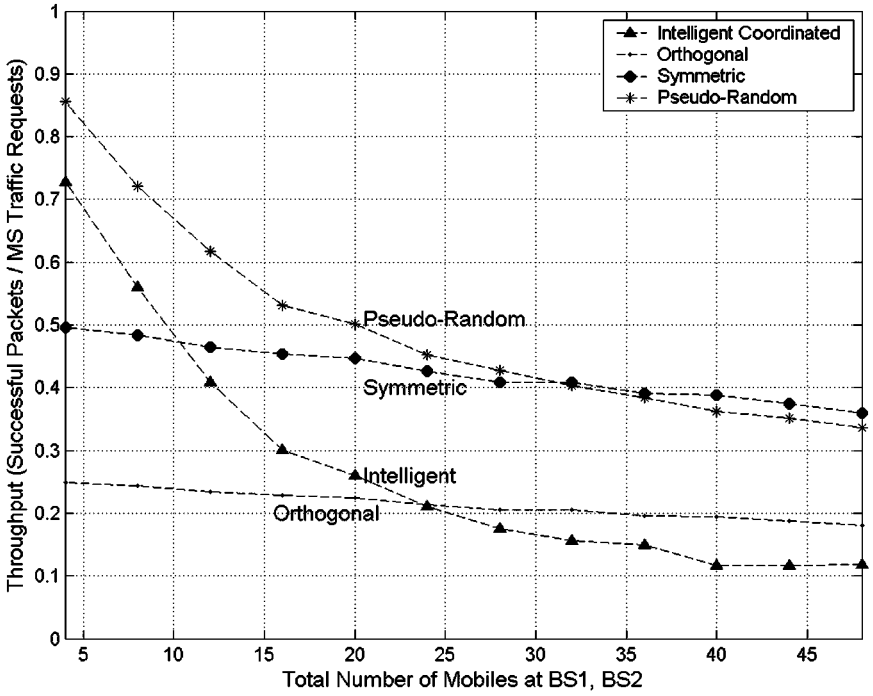

Fig. 18. Tx throughput of a two-BS system with various channel-allocation algorithms in dynamic traffic. $\alpha = 0.125, \beta \approx 0.75$ (measured), $N_{\rm ncar}/N_{\rm far} = 0.5$, $T = 8$, and time frame trials $= 1$ million).

4) intelligent coordinated-BS throughput is approximately 0.73, which is a little worse than the pseudorandom algorithm, as even though all the time slots can be allocated to Tx traffic, the algorithm limits the Tx packets allocated in the far region.

At high traffic levels, the following characteristics can be observed about the Tx throughput with the dynamic traffic model:

1) symmetric throughput is approximately 0.36 and the channel has saturated, as shown by the flat throughput function in Fig. 18;
2) orthogonal throughput is approximately 0.19, as the channel has saturated and there are half as many time

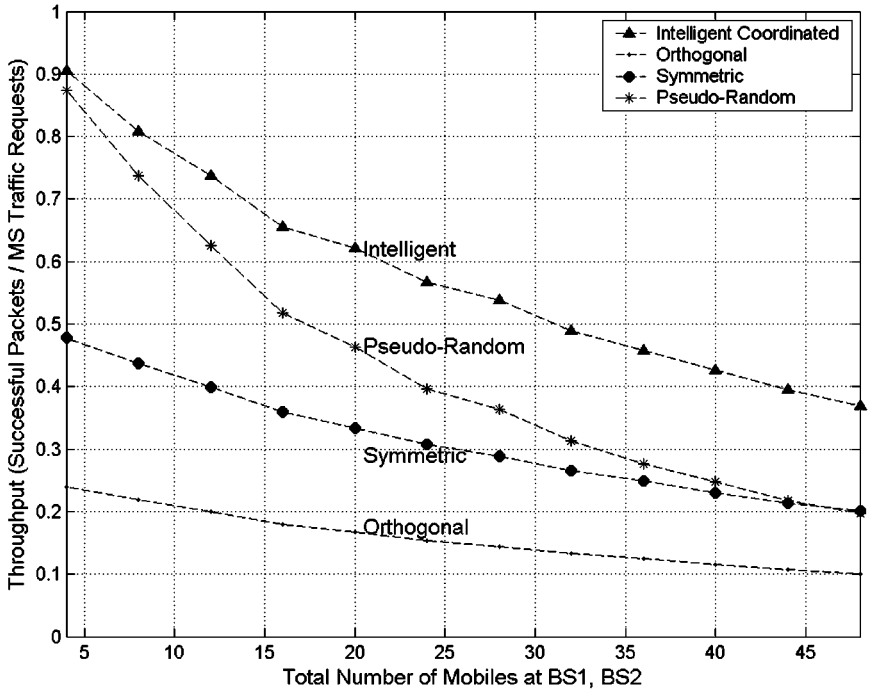

Fig. 19. Rx throughput of a two-BS system with various channel-allocation algorithms in dynamic traffic. $\alpha = 0.125$, $\beta \approx 0.75$ (measured), $N_{\rm near}/N_{\rm far} = 0.5$, $T = 8$, and time frame trials = 1 million).

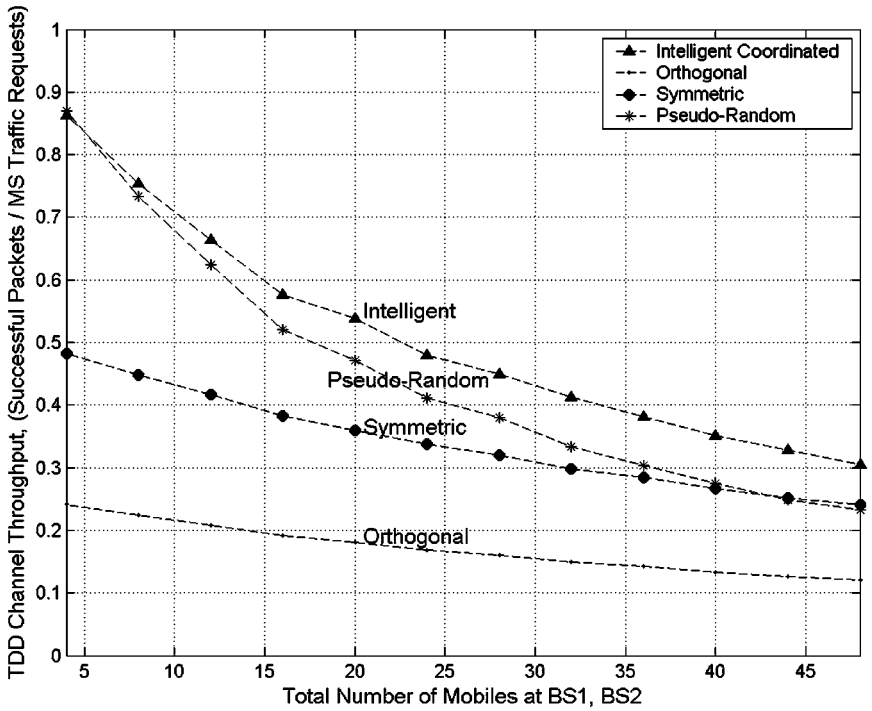

Fig. 20. Overall throughput of two-BS system with various channel-allocation algorithms in dynamic traffic. $\alpha = 0.125$, $\beta \approx 0.75$ (measured), $N_{\rm near}/N_{\rm far} = 0.5$, $T = 8$, and time frame trials = 1 million).

slots allocated to Tx packets compared to the symmetric algorithm;

3) pseudorandom throughput converges with the symmetric throughput as the pseudorandom algorithm assigns Tx packets to time slots with a 0.5 probability (see Section V-C); the symmetric algorithm allocates 50% of the time slots to Tx packets, so when the channel is saturated, the Tx throughput of both algorithms is about the same;
4) intelligent coordinated-BS throughput is poor, as the channel is saturated and the algorithm limits the allocation of Tx packets, which would otherwise cause interference blocking (see Fig. 13 and Rules C and E).

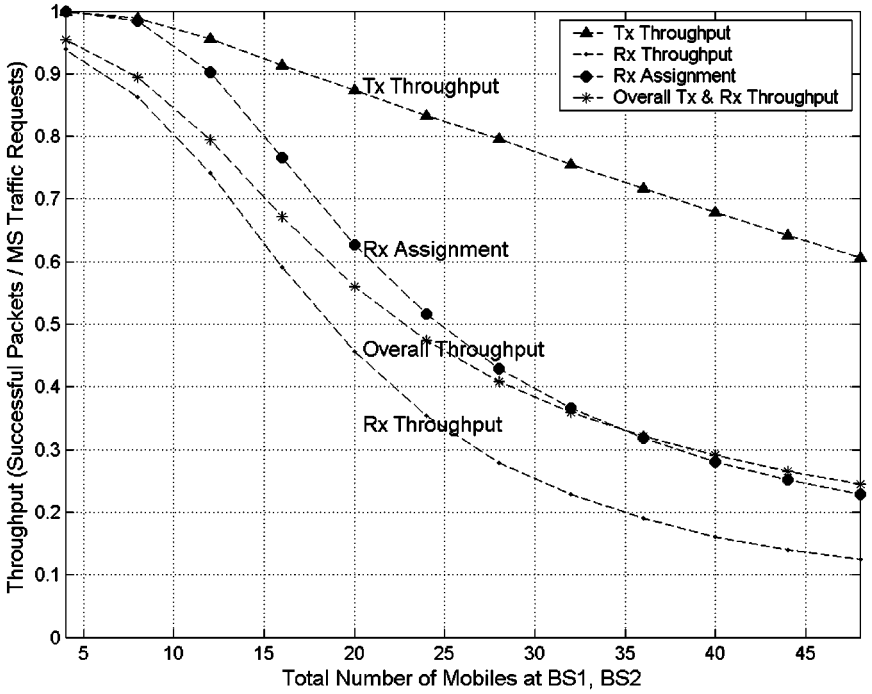

Fig. 21. Throughput of a two-BS system with pseudorandom channel-allocation in binomial traffic. $\alpha = 0.125$, $\beta = 0.75$, $N_{\rm near}/N_{\rm far} = 0.5$, $T = 8$, and time frame trials $= 100\,000$). Note that Tx interference blocking reduces Rx packet throughput by 50% below Rx assignment rate at high traffic levels.

Comparing the Tx throughput with dynamic traffic in Fig. 18 to the Tx throughput with binomial traffic in Fig. 15, it is clear that the Tx throughput is better with the binomial traffic model, particularly at low traffic levels. This is because even though the two traffic models have the same average number of packets generated per time ~ frame, the binomial model has a much larger proportion of time frames with a smaller number of Tx packets generated (as shown in Fig. 3), whereas the dynamic model generates a large number of packets per time slot per active MS, which saturates the channel even at low numbers of MSs.

Note that in the dynamic traffic model results (Figs. 18–20 and Fig. 22), β is stated as being ≈ 0.75 (measured), because in the dynamic traffic model β was a measured value that varied slightly for each simulation run. The theoretical β for the dynamic traffic model (i.e., 0.74 from Section IV-B) is dependent on the Markov state probabilities and flow sizes specified in Table III, whereas, in the binomial traffic model, the β can be directly specified as an input parameter to the binomial traffic model.

E. Rx Throughput With Dynamic Traffic

Fig. 19 shows the Rx throughput in dynamic traffic, of which the following can be observed:

1) symmetric throughput is approximately 0.5, as the channel has saturated and only half the time slots are allocated to Rx traffic;
2) orthogonal throughput is approximately 0.25, as the channel has saturated and only a quarter of the time slots are allocated to Rx traffic;
3) pseudorandom throughput is high at approximately 0.88, since all the time slots can be assigned and the Tx interference blocking is low;
4) intelligent coordinated-BS throughput is high at around 0.9 as all the time slots can be assigned to traffic and Rx packet assignment is biased.

At high traffic levels, the following can be observed about the Rx throughput with the dynamic traffic model:

1) symmetric throughput is approximately 0.2 and the channel has saturated, as shown by the flat throughput function in Fig. 18;
2) orthogonal throughput is approximately 0.1, as the channel has saturated and there are half as many time slots allocated to Rx packets compared to the symmetric algorithm;
3) pseudorandom throughput converges with the symmetric throughput (to approximately 0.2) as the pseudorandom algorithm suffers from Tx interference blocking;
4) intelligent coordinated-BS throughput is highest at around 0.37, as even though the channel is saturated, the algorithm biases the allocation of the Rx packets generated.

F. Overall Throughput With Dynamic Traffic

Fig. 20 shows the overall throughput with dynamic traffic. The following observations can be made:

1) symmetric throughput is approximately 0.5 at low traffic, reducing to 0.24 at high traffic, as the channel has saturated and only half the time slots are allocated to Rx traffic and Tx traffic, whereas the large flow sizes in the dynamic traffic model have all the time slots filled with either Tx or Rx packets;

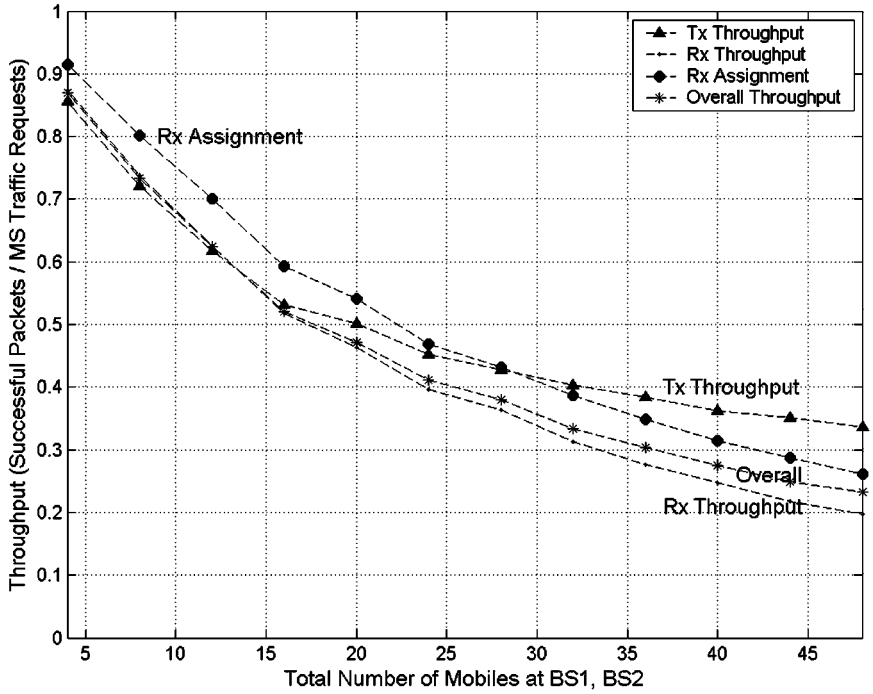

Fig. 22. Throughput of a two-BS system with pseudorandom channel allocation in dynamic traffic. $\alpha = 0.125$, $\beta \approx 0.75$ (measured), $N_{\rm near}/N_{\rm far} = 0.5$, $T = 8$, and time frame trials $= 1$ million).

2) orthogonal throughput is around 0.25 at low traffic, reducing to 0.12 at high traffic, as the channel has saturated and only a quarter of the time slots are allocated to Rx traffic;
3) pseudorandom throughput is approximately 0.87 at low traffic, reducing to 0.23 at high traffic and converging to the same throughput as the symmetric throughput due to the Tx interference blocking;
4) intelligent coordinated-BS throughput is the best of all the algorithms as it maximizes the overall packet assignment, while avoiding Tx interference blocking.

Interestingly, the results indicate that pseudorandom channel-allocation performs well in low traffic and at least as good as symmetric fixed channel allocation in high traffic, even with the receive interference blocking.

G. Assignment Versus Throughput with Pseudorandom Channel Allocation

Fig. 21 shows the assignment and throughput for pseudorandom assignment in binomial traffic. At high traffic levels, the Rx assignment is 23%, whereas the Rx throughput is 12% due to adjacent BS Tx interference blocking.

Note that the Tx assignment is much higher than the Rx assignment, since there are far fewer Tx packets generated per time frame (with $\beta = 0.75$) and the pseudorandom algorithm assigns Tx packets to time slots with a 0.5 probability.

Fig. 22 shows the assignment and throughput probabilities for pseudorandom assignment in dynamic traffic. Here, there is less of a difference between the Tx and Rx throughputs as the traffic generated by the dynamic model is either almost all idle or active packets and the active packets are either all Tx or all Rx packets, but not often both, except at high traffic levels. Thus, the main blocking is due to the lack of available time slots, not the adjacent BS Tx interference.

VIII. Conclusion

In this paper, we have developed a two-BS interference model and a dynamic Markov event-driven traffic model representative of wireless Internet traffic. An equivalent binomial model was developed to derive the theoretical performance of fixed and pseudorandom channel-allocation algorithms and to validate the throughput-simulation model. The characteristic differences between the two traffic models were observed and showed the limitations of the binomial model, particularly with respect to message-flow length and uplink–downlink traffic dynamics. For active MSs, the dynamic traffic model generated much larger numbers of packets per time frame than the binomial model, even at low MS activity factors.

It was seen that the throughput performance is highly dependent on the traffic source and that the intelligent coordinated algorithm provided the best overall throughput with both binomial and dynamic traffic models and at all traffic levels.

The pseudorandom algorithm performed surprisingly well even in dynamic traffic, because all of the time slots could be allocated to packet requests and, due to the low MS activity α and large message size used in the simulations, the interference blocking was mitigated, particularly at low traffic levels. However, it is clear that the pseudorandom allocation will perform poorly at high traffic levels when there is a large difference in β between the two adjacent BSs, i.e., one BS having a high number of Rx packets assigned and the adjacent BS having a high number of Tx packets assigned.

The symmetric allocation algorithm works reasonably well, especially when the number of Tx and Rx time slots assigned

is matched to the β of the traffic model, but the algorithm is still limited by the fixed time-slot allocation with the dynamic traffic model. The orthogonal allocation algorithm only works well with the binomial model at low traffic levels, as there are insufficient time slots allocated to support the traffic load.

Further research is necessary to determine whether a dynamic wireless Internet traffic model that does not include the flow size distribution for each traffic type is sufficiently realistic to simulate the performance of DCA algorithms. Additionally, the simulation model needs to be expanded to support small multi-BS multisector networks with a space–time multiple-input–multiple-output (MIMO) wireless propagation channel.

ACKNOWLEDGMENT

The authors would like to thank J. Madden, Manager of Network Operations, Academic Computing Services, UCSD, for supplying the aggregated traffic logs for the UCSD 802.11b wireless network. They would also like to thank A. Balachandran, G. Varghese, and G. Voelker for their valuable comments and suggestions regarding the Internet traffic measurements and models.

REFERENCES

[1] IEEE Std 802.11b-1999, 2000. Supplement to ANSI/IEEE Std 802.11, 1999 ed..
[2] C. You and K. Chandra, "Time series models for internet data traffic," in *Proc. Conf. Local Computer Networks*, Oct. 1999, pp. 164–171.
[3] W. E. Leland and M. S. Taqqu *et al.*, "On the self-similar nature of ethernet traffic (extended version)," *IEEE/ACM Trans. Networking*, vol. 2, pp. 1–15, Feb. 1994.
[4] V. H. MacDonald, "The cellular concept," *Bell Syst. Tech. J.*, vol. 58, no. 1, pp. 15–41, 1979.
[5] J. R. Boucher, *Traffic System Design Handbook*, ser. Telecommunications Handbook. Piscataway, NJ: IEEE Press, 1993.
[6] G. Ostermayer, P. Slanina, and C. Holzl *et al.*, "Scheduling algorithm for UTRA TDD mode," in *Proc. IEEE/AFCEA EUROCOMM'00*, 2000, pp. 212–216.
[7] H. Holma and A. Toskala, *WCDMA for UMTS—Radio Access for Third Generation Mobile Communications*. New York: Wiley, 2000.
[8] M. Haardt, A. Klein, and R. Koehn *et al.*, "The TD-CDMA based UTRA TDD mode," *IEEE J. Select. Areas Commun.*, vol. 18, pp. 1375–1385, Aug. 2000.
[9] C. X. Fan, H. H. Chen, and W. W. Lu, "China's perspectives on 3G mobile communications and beyond: TD-SCDMA technology," *IEEE Wireless Commun.*, vol. 9, pp. 48–59, Apr. 2002.
[10] J. Terry and J. Heiskala, *OFDM Wireless LANs: A Theoretical and Practical Guide*, 1st ed. Indianapolis, IN: Sams, 2001.
[11] M. Casoni and M. L. Merani, "Erlang capacity of a TDD-TD/CDMA architecture supporting heterogeneous traffic," *IEEE Commun. Lett.*, vol. 5, Dec. 2001.
[12] M. Qingyu, W. Wenbo, Y. Dacheng, and W. Daqing, "An analysis of the interference in the TDD-CDMA system," in *Proc. TENCON'00*, vol. 1, Sept. 2000, pp. 333–337.
[13] W. Y. C. Lee, *Mobile Communication Design Fundamentals*. New York: Wiley, 1993.
[14] G. Boggia and P. Camarda, "Modeling dynamic channel allocation in multicellular communication networks," *IEEE J. Select Areas Commun.*, vol. 19, pp. 2233–2242, Nov. 2001.
[15] E. Del Re, R. Fantacci, and G. Giambene, "Handover and dynamic channel allocation techniques in mobile cellular networks," *IEEE Trans. Veh. Technol.*, vol. 44, pp. 229–237, May 1995.
[16] I. Katzela and M. Nagshineh, "Channel assignment schemes for cellular mobile telecommunication systems: A comprehensive survey," *IEEE Pers. Commun.*, pp. 10–31, June 1996.
[17] D. Everitt and D. Manfield, "Performance analysis of cellular mobile communication systems with dynamic channel assignments," *IEEE J. Select. Areas Commun.*, vol. 7, pp. 1172–1180, Oct. 1989.
[18] Y. Argyropoulos and S. Jordan, "Dynamic channel allocation in interference-limited cellular systems with uneven traffic distribution," *IEEE Trans. Veh. Technol.*, vol. 48, pp. 224–232, Jan. 1999.
[19] J. S. Blogh, P. J. Cherriman, and L. Hanzo, "Adaptive antenna array assisted DCA techniques," *IEEE J. Select. Areas Commun.*, vol. 19, pp. 305–311, Feb. 2001.
[20] J. Perez-Romero and R. Agusti *et al.*, "Packet transmission strategies to provide quality of service," in *Proc. 12th IEEE Int. Symp. PIMRC'01*, , vol. 2, Sept. 2001, pp. 147–151.
[21] A. Kramling, M. Scheibenbogen, and B. Walke, "Dynamic channel allocation in wireless atm networks," *Wireless Networks*, vol. 6, no. 5, pp. 381–389, 2000.
[22] W. S. Jeon and D. G. Jeong, "Comparison of timeslot assignment allocation strategies for CDMA/TDD systems," *IEEE J. Select. Areas Commun.*, vol. 18, pp. 1271–1278, July 2000.
[23] H. Haas and S. Mclaughlin, "A dynamic channel assignment algorithm for a hybrid TDMA/CDMA-TDD interface using the novel TS-opposing technique," *IEEE J. Select. Areas Commun.*, vol. 19, pp. 1831–1846, Oct. 2001.
[24] M. R. Garey and D. S. Johnson, *Computers and Intractability: A Guide to the Theory of NP-Completeness*. San Francisco, CA: W. H. Freeman, 1979.
[25] J. Gordon, "Pareto process as a model of self-similar traffic," in *Proc. IEEE GLOBECOM'95*, vol. 3, Nov. 14–16, 1995, pp. 2232–2236.
[26] N. L. Johnson and S. Kotz, *Urn Models and Their Application*. New York: Wiley, 1977.
[27] W. Cooper, J. Zeidler, and S. McLaughlin, "Performance analysis of slotted random access channels for W-CDMA systems in Nakagami fading channels," *IEEE Trans. Veh. Technol.*, vol. 51, pp. 411–424, May 2002.

William Cooper (S'91) received the B.Sc. (Hons.) degree in electronic engineering from the University of Wales, Swansea, and the M.Sc. degree in electrical engineering from the University of California at San Diego (UCSD), La Jolla, in 1985 and 1998, respectively. He is currently working toward the Ph.D. degree at the UCSD.

His research interests include wide-band code-division multiple-access (CDMA) communications, adaptive array processing, and propagation aspects of mobile radio systems.

James R. Zeidler (M'76–SM'84–F'94) is a Research Scientist and Senior Lecturer, Electrical and Computer Engineering Department, the University of California at San Diego (UCSD), La Jolla. From 1988 to 2003, he was an Adjunct Professor at UCSD. From 1974 to 2003, he also was a Scientist with the Space and Naval Warfare Systems Center, San Diego, CA. His research interests include communications signal processing, adaptive signal processing, array processing, and mobile *ad hoc* networks.

Dr. Zeidler was an Associate Editor of the IEEE TRANSACTIONS ON SIGNAL PROCESSING from 1991 to 1994. He received the Lauritsen–Bennett Award for achievement in science in 2000 and the Navy Meritorious Civilian Service Award in 1991. He was a Corecipient of the award for the Best Unclassified Paper at the IEEE Military Communications Conference in 1995.

Robert R. Bitmead (S'76–M'79–SM'86–F'91) was born in Sydney, Australia, in 1954. He received the B.Sc. degree in applied mathematics from the University of Sydney and the M.E. and Ph.D. degrees from the University of Newcastle, Callaghan, Australia, in 1976, 1977, and 1979, respectively.

He has held faculty positions at the Australian National University, the University of Newcastle, and James Cook University of North Queensland and visiting positions at Cornell University, Ithaca, NY; the University of Louvain, Belgium; and l'Institut National de Recherche en Informatique et en Automatique, Sophia-Antipolis, France. He has been with the faculty of the University of California at San Diego, La Jolla, since 1999, where he currently is Professor of mechanical and aerospace engineering. His research interests encompass adaptive systems in control, signal processing and telecommunications, stochastic processes, and multivariable and predictive control.